



The Mammalian Ecdysoneless Protein Interacts with RNA Helicase DDX39A To Regulate Nuclear mRNA Export

Irfana Saleem,^{a,b} Sameer Mirza,^a Aniruddha Sarkar,^a Mohsin Raza,^a Bhopal Mohapatra,^a Insha Mushtaq,^c Jun Hyun Kim,^{a,*} Nitish K. Mishra,^a Mansour A. Alsaleem,^{g,*} Emad A. Rakha,^g Fang Qiu,^{d,f} Chittibabu Guda,^{a,f}  Hamid Band,^{a,b,c,e,f}  Vimla Band^{a,b,f}

^aDepartment of Genetics, Cell Biology and Anatomy, University of Nebraska Medical Center, Omaha, Nebraska, USA

^bDepartment of Biochemistry and Molecular Biology, University of Nebraska Medical Center, Omaha, Nebraska, USA

^cDepartment of Pathology and Microbiology, University of Nebraska Medical Center, Omaha, Nebraska, USA

^dDepartment of Biostatistics, University of Nebraska Medical Center, Omaha, Nebraska, USA

^eEppley Institute for Research in Cancer and Allied Diseases, University of Nebraska Medical Center Omaha, Nebraska, USA

^fFred & Pamela Buffett Cancer Center, University of Nebraska Medical Center, Omaha, Nebraska, USA

^gDepartment of Pathology, School of Medicine, University of Nottingham, Nottingham, United Kingdom

Irfana Saleem and Sameer Mirza are co-first authors. Irfana Saleem initiated the project and contributed both intellectually and experimentally. Sameer Mirza completed the project and carried out studies for manuscript revision.

ABSTRACT The mammalian orthologue of ecdysoneless (ECD) protein is required for embryogenesis, cell cycle progression, and mitigation of endoplasmic reticulum stress. Here, we identified key components of the mRNA export complexes as binding partners of ECD and characterized the functional interaction of ECD with key mRNA export-related DEAD BOX protein helicase DDX39A. We find that ECD is involved in RNA export through its interaction with DDX39A. ECD knockdown (KD) blocks mRNA export from the nucleus to the cytoplasm, which is rescued by expression of full-length ECD but not an ECD mutant that is defective in interaction with DDX39A. We have previously shown that ECD protein is overexpressed in ErbB2⁺ breast cancers (BC). In this study, we extended the analyses to two publicly available BC mRNA The Cancer Genome Atlas (TCGA) and Molecular Taxonomy of Breast Cancer International Consortium (METABRIC) data sets. In both data sets, ECD mRNA overexpression correlated with short patient survival, specifically ErbB2⁺ BC. In the METABRIC data set, ECD overexpression also correlated with poor patient survival in triple-negative breast cancer (TNBC). Furthermore, ECD KD in ErbB2⁺ BC cells led to a decrease in ErbB2 mRNA level due to a block in its nuclear export and was associated with impairment of oncogenic traits. These findings provide novel mechanistic insight into the physiological and pathological functions of ECD.

KEYWORDS ECD, ecdysoneless, hSGT1, ErbB2, RNA processing, RNA export, RNA splicing, RNA helicase, oncogenesis

Eukaryotic gene function requires precise coordination of transcription with mRNA processing, including splicing, capping, and polyadenylation, and efficient export through the nuclear pore complex to transfer the mRNAs to the cytoplasm where the machinery for translation resides (1–5). The kinetics and efficiency of the export of a mature mRNA from the nucleus to the cytoplasm require elaborate export machinery (4, 6–8). Key components of this machinery include the nuclear pore complex proteins (NPCs), RNA-binding/non-RNA-binding adaptor proteins, chaperones, and cochaperones inside the nucleus, which help the mRNAs to transverse the nuclear envelope and reach the cytoplasmic compartment (1, 2, 8–10). Two major mRNA export pathways are the nuclear RNA export factor 1 (NXF1)–NTF2-related export protein 1 (NXT1)-mediated bulk mRNA export pathway and the CRM1/XPO1-mediated selective mRNA export pathway

Citation Saleem I, Mirza S, Sarkar A, Raza M, Mohapatra B, Mushtaq I, Kim JH, Mishra NK, Alsaleem MA, Rakha EA, Qiu F, Guda C, Band H, Band V. 2021. The mammalian ecdysoneless protein interacts with RNA helicase DDX39A to regulate nuclear mRNA export. *Mol Cell Biol* 41: e00103-21. <https://doi.org/10.1128/MCB.00103-21>.

Copyright © 2021 Saleem et al. This is an open-access article distributed under the terms of the [Creative Commons Attribution 4.0 International license](https://creativecommons.org/licenses/by/4.0/).

Address correspondence to Hamid Band, hband@unmc.edu, or Vimla Band, vband@unmc.edu.

*Present address: Jun Hyun Kim, Molecular Biology Program, Memorial Sloan-Kettering Cancer Center, New York, New York, USA; Mansour A. Alsaleem, Department of Applied Medical Sciences, Onizah Community College, Qassim University, Qassim, Saudi Arabia.

Received 10 March 2021

Returned for modification 4 April 2021

Accepted 19 April 2021

Accepted manuscript posted online

3 May 2021

Published 23 June 2021

(11–22). Both export pathways function in association with multiple adaptor proteins that associate with the mRNAs to form the mature messenger ribonucleoproteins (mRNPs) and help dock the mRNAs to the NPC channels for efficient export (4, 6, 18, 23, 24). The CRM1-mediated mRNA export pathway is more selective and facilitates the export of ribosomal RNAs, viral RNAs, U-snrRNA, and other mRNAs using known as well as undefined adaptor proteins (1–8, 10, 17, 25–27).

Given the fundamental role of the mRNA export pathway in cell physiology and the importance of regulated mRNA transport under various physiological conditions and during pathological situations (2, 28, 29), the identification of novel components of the mRNA export machinery is of great interest. Here, we describe the mammalian ecdysoneless (ECD) protein as a novel structural and functional component of the mRNA export machinery.

The mammalian ECD is the highly conserved orthologue of *Drosophila* ecdysoneless (Ecd) whose mutations lead to developmental arrest due to loss of the metamorphosis-associated ecdysone hormone secretion during early development (50). *Drosophila* Ecd also functions cell autonomously in embryonic cell survival and was previously found to interact with the spliceosome factor pre-mRNA processing 8 (Prp8; orthologue of the mammalian PRPF8) (50), and loss of Prp8 or Ecd led to defective splicing of the ecdysone biosynthetic enzyme CYP307A2/spookier (spok) pre-mRNA, providing a basis for the metamorphosis defects in *ecd* mutant flies (30). Notably, human ECD could compensate for loss of *Drosophila* Ecd for this function.

We have previously shown that germ line deletion of *Ecd* in mice leads to early embryonic lethality and that recombination-mediated deletion of *Ecd* in mouse embryonic fibroblasts (MEFs) from *Ecd^{flox/flox}* (*Ecd^{fl/fl}*) mice or the short hairpin RNA (shRNA)-mediated knockdown of ECD in human mammary epithelial cells leads to G₁ cell cycle arrest, indicating an essential role of mammalian ECD in cell cycle progression (31). Recently, using depletion and overexpression approaches, we uncovered a role of ECD in mitigating endoplasmic reticulum stress through ECD-dependent attenuation of the PRKR-like endoplasmic reticulum kinase (PERK) branch of the unfolded protein response (32). We and others have shown that ECD interacts with the R2TP cochaperone complex (consisting of RUVBL1, RUVBL2, RPAP3, and PIH1D1 proteins), which functions in the assembly and remodeling of multimeric protein-RNA complexes, such as the U5 small nuclear ribonucleoprotein (snRNP) complex (33–37). Notably, mammalian PRPF8 also interacts with ECD (37), and another study found ECD, PRPF8, and R2TP subunits in a single complex (35). These studies have begun to point to potential roles of ECD in RNA biogenesis.

While the crystal structure of ECD is not known, our previous analysis using circular dichroism measurements and sequence analysis software showed that the majority of ECD is composed of α -helices and that the C-terminal 100 or so amino acids are disordered in the absence of binding partners. Furthermore, small-angle X-ray scattering (SAXS) analysis showed that the first 400 residues are globular and the next 100 residues are in an extended cylindrical structure (33), suggesting ECD acts like a structural hub or scaffolding protein in its associations with protein partners.

The importance of understanding the mechanism of how ECD functions is further highlighted by studies by us and others that have demonstrated ECD overexpression in several human cancers, such as those of pancreas, breast, and gastric tumors (38–41). We have shown that ECD overexpression in breast cancer patients correlates with poor prognosis and shorter survival, especially in the ErbB2⁺ breast cancer subtype (39). These studies support the likelihood of ECD's role in promoting oncogenesis, a possibility supported by the ability of overexpressed ECD to cooperate with mutant H-Ras to oncogenically transform nontumorigenic immortal human mammary epithelial cells (42).

Here, we identify components of the mRNA export machinery as interacting partners of ECD and show that ECD regulates mRNA export. We previously showed that ECD protein is overexpressed in ErbB2⁺ breast cancers (BC). Furthermore, using The

Cancer Genome Atlas (TCGA) and Molecular Taxonomy of Breast Cancer International Consortium (METABRIC) data sets, we show ECD mRNA overexpression correlates with short patient survival, specifically in ErbB2⁺ as well as triple-negative breast cancer (TNBC) patients, and serves as an independent prognostic marker. In ErbB2⁺ BC cells, ECD regulates ErbB2 mRNA export and stability and is required for ErbB2⁺ breast cancer cell proliferation, anchorage-independent growth, migration, and invasion. Thus, our findings provide new mechanistic insight into the physiological role of ECD and a potential basis for how overexpressed ECD may promote oncogenesis.

RESULTS

ECD interacts with components of the mRNA export machinery. To gain insights into mechanisms by which mammalian ECD functions, we used two complementary approaches to identify ECD-associated cellular proteins. In one approach, we used a recombinant ECD protein with an N-terminal glutathione transferase (GST) and a C-terminal FLAG tag in an *in vitro* tandem affinity purification approach to identify cellular proteins that specifically bind to ECD; in the second approach, we expressed a FLAG-tagged ECD in HEK-293T cells and carried out affinity purification of ECD-associated proteins. In both approaches, mass spectrometry was used to identify ECD-associated proteins. A number of known as well as novel interacting proteins involved in various cellular processes were identified, including proteins involved in transcription, RNA processing, translation, ATP transport, cytoskeleton, metabolism, kinase pathways, and vesicle-mediated transport (see Table S1A in the supplemental material). Significantly, ECD-associated protein complexes from *in vitro* and *in vivo* approaches (listed above) include multiple proteins involved in mRNA export, such as U5 small nuclear ribonucleoprotein component (EFTUD2), BRR2, DDX39A/B, and LRPPRC as well as PRPF8 (Table S1A and B, highlighted in bold font), which was previously implicated in ECD's role in mRNA splicing in *Drosophila* (30) and whose association with ECD in mammalian cells we reported previously (37).

In view of a lack of previous linkage between ECD and mRNA export, studies here focused on further characterization of the interaction of ECD with DDX39A RNA helicase, an ECD-associated protein previously established as a critical player in mRNA export (43–47). We have already shown that ECD localizes to both nucleus and cytoplasm and harbors a very strong CRM1-mediated nuclear export signal and that, with leptomycin B treatment, exogenous ECD is retained in the nucleus (48). To confirm the interactions identified by mass spectrometry, we first carried out immunoprecipitations (IPs) of endogenous proteins followed by Western blotting (WB) for the potential interacting partners. IP from lysates of HEK-293T cells with antibodies against ECD (Fig. 1A) or DDX39A (Fig. 1B) versus rabbit (rlgG) or mouse (mlgG) IgG (as negative controls) followed by WB for ECD, DDX39A, or Casitas B-lineage lymphoma (CBL; an expected non-interacting control) showed that ECD coimmunoprecipitated with DDX39A and ALY, the latter a known interacting partner of DDX39A (49) that served as a positive control. Next, we expanded our analyses by carrying ECD, LRPPRC, CRM1, ALY, or IgG IPs from lysates of HEK-293T (Fig. 1C and D) or MCF10A (a spontaneously immortalized mammary epithelial cell line) (Fig. 1E) cell lysates and subjected these to WB with antibodies against CRM1, LRPPRC, ALY, DDX39A, or ECD (Fig. 1C). Conversely, we performed IP with anti-ECD or anti-DDX39A antibodies followed by WB with antibodies against the various mRNA export-associated proteins (Fig. 1D and E). These analyses demonstrated the association of endogenous ECD with DDX39A and with its associated protein complex (ALY, LRPPRC, and CRM1) in both cell lines (Fig. 1A to E). Co-IP of CRM1 served as a positive control for LRPPRC IP, as reported earlier (24), and co-IP of ALY served as a positive control for DDX39A IP.

In the second approach to confirm the interaction of ECD with DDX39A, we carried out pulldown experiments with GST fusion protein of ECD (amino acids 1 to 644) or GST alone (negative control) from lysates of HEK-293T cells transiently transfected to overexpress FLAG-DDX39A or FLAG-RUVBL1 (known binding partner of ECD) (37). WB

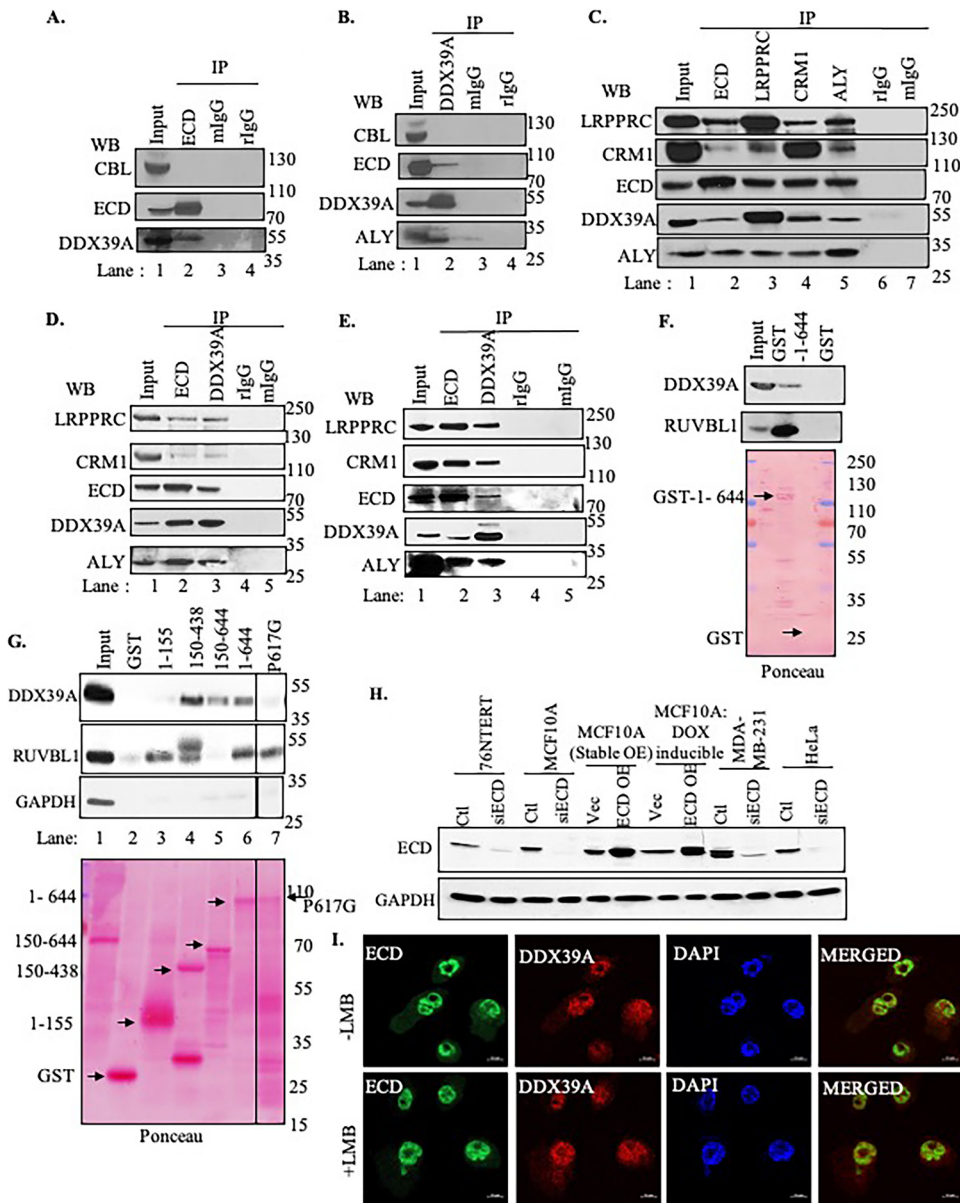


FIG 1 ECD interacts with DDX39A and other components of the mRNA export machinery. (A to E) HEK-293T (A to D) or MCF10A (E) cell lysates were immunoprecipitated (IP) with the antibodies indicated at the top, followed by Western blotting (WB) with the antibodies shown on the left. ALY and CRM1 were used as positive controls. CBL, mouse IgG (mlgG), and rabbit IgG (rlgG) were used as negative controls; 100-μg aliquots of lysate protein were used in the input lane. (F) Twenty micrograms of GST (negative control) or GST fusion with full-length ECD (1 to 644) was incubated with 1 mg of protein lysate from HEK-293T cells transfected with FLAG-tagged RUVBL1 or FLAG-tagged DDX39A, and the GST pull-down proteins were analyzed by Western blotting with the indicated antibodies. The membrane was stained with Ponceau S to visualize the GST fusion proteins to assess comparable fusion protein use for pull-downs (indicated by arrows). (G) GST or GST fusion with full-length ECD (1 to 644) or indicated ECD mutants were incubated with protein lysate of HEK-293T cells transiently transfected with FLAG-tagged-DDX39A and FLAG-tagged RUVBL1, and the bound proteins were analyzed by Western blotting with the indicated antibodies. The membrane was stained with Ponceau S to visualize the GST fusion proteins (indicated by arrows). The experiment shown is a representative of at least three repeats with comparable results. (H) To validate ECD commercial antibody, Western blotting was performed in various cell lysates from control and ECD siRNA-treated MCF10A, 76NERT, MDA-MB-231 and HeLa cells and ECD-overexpressing MCF10A stable as well as DOX-inducible (as indicated); glyceraldehyde-3-phosphate dehydrogenase (GAPDH) was used as loading control. (I) ECD colocalizes with DDX39A in the nucleus. MCF10A cells untreated or treated with 20 ng/μl of leptomycin B (LMB) for 4 h and fixed in 4% paraformaldehyde (PFA) were subjected to immunofluorescence staining using anti-ECD rabbit polyclonal and anti-DDX39 mouse monoclonal antibodies followed by imaging using 63× Zeiss confocal microscope (scale bars, 10 μm).

of pulldowns confirmed the binding of ECD to DDX39A as well as to RUVBL1 (Fig. 1F). Next, to assess the regions of ECD that are required for binding to DDX39A, we used pulldowns with the GST fusion protein of full-length ECD (1 to 644) versus its various fragments (amino acids 1 to 155, 150 to 438, or 150 to 644) and ECD-P617G, which has single amino acid change (glycine in place of a proline conserved in multiple organisms and also known to cause molting defects in *Drosophila* upon mutation to other amino acid [50]). The deletion mutants ECD₁₅₀₋₄₃₈ and ECD₁₅₀₋₆₄₄ pulled down similarly to full-length ECD (FL-ECD; amino acids [aa] 1 to 644), while an N-terminal ECD fragment (ECD₁₋₁₅₅) failed to bind to DDX39A (Fig. 1G), suggesting that the ECD region encompassing amino acids 150 to 438 is required for interaction with DDX39A. Notably DDX39A binding was abolished in the ECD-P617G mutant (Fig. 1G and Fig. S1); however, the single-amino-acid-change ECD mutant retained the ability to associate with RUVBL1, arguing against gross misfolding of this protein. The inability of this mutant to bind DDX39A suggests a potential modulation of the ECD-DDX39A interaction by the C-terminal region harboring the mutation, but the mechanism of such modulation remains unclear.

In addition, we also performed immunofluorescence analysis to assess if ECD is colocalized in the nucleus with DDX39A. As reported previously, ECD shuttles between the nucleus and cytoplasm, and leptomycin B treatment blocks nuclear export of ECD (48, 51). As our monoclonal antibody (39, 51) recognizes the cytoplasmic pool of ECD, we used a commercially available antibody against ECD. We first validated the specificity of this antibody in WB (Fig. 1H), followed by assessing if ECD colocalizes with DDX39A. These experiments showed leptomycin B treatment of cells results in predominantly nuclear localization of ECD, which colocalized with DDX39A (Fig. 1I).

As DDX39A is an RNA-binding protein, we further analyzed whether associations of DDX39A with ECD are RNA dependent by treating cell lysates with either RNase or Benzonase followed by IP/WB. We observed that ECD interaction with DDX39A is RNA independent (Fig. 2A to D). In these experiments, we used telomerase reverse transcriptase (TERT) and dyskerin association, a known RNA-dependent interaction, as our positive control (Fig. 2C and D). Furthermore, our previous studies have shown ECD is a phosphoprotein, and casein kinase 2 phosphorylates ECD at multiple sites (37). To assess if phosphorylation of ECD is required for its interaction with DDX39A, we used two phosphomutants of ECD and analyzed their association with DDX39A. As shown in Fig. 2E, phospho-deficient mutants associated with DDX39A similarly to wild-type ECD. Thus, ECD phosphorylation is not required for its association with DDX39A.

Taken together, our analyses established that ECD interacts with DDX39A and its associated nuclear export protein complex.

ECD regulates nuclear mRNA export to the cytoplasm. The interaction of ECD with DDX39A and associated proteins involved in mRNA export supported a potential functional role of ECD in regulating mRNA export from the nucleus to the cytoplasm. To address this possibility, we first examined the impact of ECD knockdown (KD) on mRNA export using fluorescence *in situ* hybridization (FISH) analysis of poly(A) mRNAs (26, 45, 52). Immortal mammary epithelial cell lines MCF10A and 76NTERT were transfected with control small interfering RNA (siRNA) or with two independent siRNAs against ECD or DDX39A (used as a positive control), and ECD or DDX39A KD was confirmed by Western blotting (Fig. 3A and D). FISH analysis of the relative abundance of nuclear versus cytoplasmic poly(A) mRNA revealed that DDX39A KD led to increased nuclear relative to cytoplasmic poly(A) mRNA signals in both cell lines, as expected (52). Notably, similar to that seen with DDX39A KD, ECD KD also led to a significant increase in nuclear poly(A) mRNA signals (Fig. 3B and E). Quantitation of the nuclear/cytoplasmic ratio of poly(A) mRNA FISH signals in 100 or more cells confirmed the nuclear accumulation of mRNA upon ECD KD (Fig. 3C and F).

To further validate the negative impact of ECD KD on poly(A) mRNA export, we utilized *Ecd^{fl/fl}* mouse embryonic fibroblasts (MEFs) (31, 32) infected with adenoviruses encoding either green fluorescent protein (GFP) (control; expressed in cytoplasm and

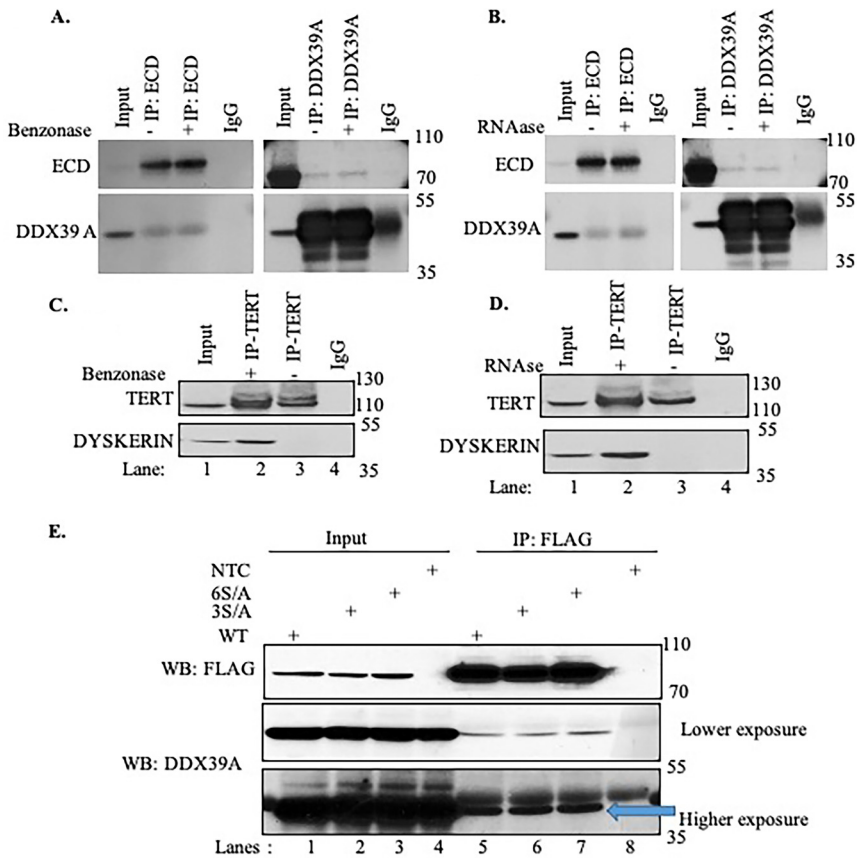


FIG 2 RNA-independent interaction of ECD with DDX39A. (A to D) MCF10A cell lysates treated with Benzonase/RNase were immunoprecipitated (IP) with the antibodies indicated at the top, followed by Western blotting (WB) with the antibodies shown on the left. TERT and dyskerin were used as positive controls. Mouse IgG (mIgG) and rabbit IgG (rIgG) were used as negative controls; 2% aliquots of lysate protein were used in the input lanes. (E) Phosphorylation-independent interaction of ECD with DDX39A. 293T cells were transfected with FLAG-tagged WT (wild-type) ECD or FLAG-tagged ECD phosphorylation site mutants 3S/A (503S/A, 505S/A, and 518S/A) and 6S/A (503S/A, 505S/A, 518S/A, 572S/A, 579S/A, and 584S/A) or untreated (nontransfected cells [NTC]). Cell lysates were immunoprecipitated (IP) with anti-FLAG antibody coupled to M2 FLAG-agarose beads (Sigma-Aldrich), followed by Western blotting (WB) with the antibodies shown on the left; 2% aliquots of lysate protein were used in the input lanes. Blue arrow indicates the DDX39A band at higher exposure.

nucleus) or GFP-Cre recombinase (nucleus targeted) to induce the deletion of floxed *Ecd* (31). Western blotting confirmed the marked depletion of ECD expression in GFP-Cre versus that in the control GFP adenovirus-infected MEFs (Fig. 3G), and immunofluorescence analysis for GFP confirmed the expression of control GFP in both cytoplasm and nucleus and that of GFP-Cre in the nucleus (Fig. 3H). Notably, compared to a more uniform nuclear and cytoplasmic distribution in GFP-expressing control MEFs, a substantial nuclear accumulation of poly(A) mRNA was observed in GFP-Cre (Ecd-deleted) MEFs (Fig. 3H). Quantification of the nuclear/cytoplasmic ratio of poly(A) mRNA FISH signals from 25 cells revealed a significant impact of *Ecd* deletion (Fig. 3I). Collectively, these analyses support the conclusion that ECD is required for efficient export of poly(A) mRNA from the nucleus to the cytoplasm.

ECD is involved in DDX39A-dependent mRNA export. Given our findings that ECD interacts with DDX39A and is required for mRNA export, we wished to examine if the ECD-DDX39A interaction is functionally important for the mRNA export function of ECD. First, we assessed if ECD KD had any impact on the levels DDX39A and other mRNA export-related proteins. ECD KD did not affect the levels or localization of DDX39A or its associated partners (data not shown). Next, we compared the ability of

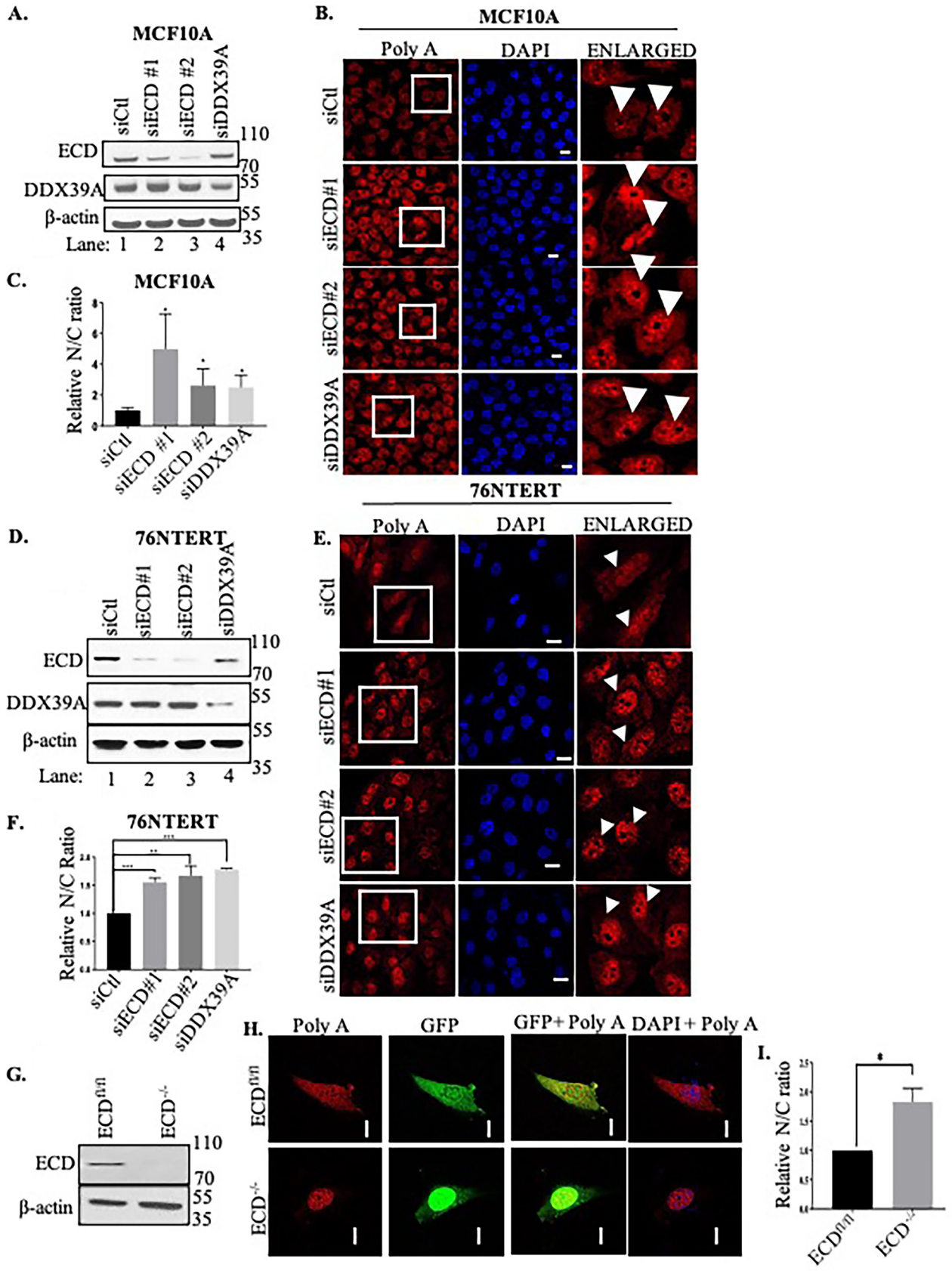


FIG 3 ECD KD decreases poly(A) mRNA export from the nucleus to the cytoplasm. (A to F) RNA FISH analysis in MCF10A (A to C) and 76NTERT (D to F) cells with control siRNA (Ctl; as a negative control), two independent siECDs (number 1 and number 2), or siDDX39A (as a positive control).

(Continued on next page)

exogenous ECD or its DDX39A-noninteracting mutant P617G to rescue the defective mRNA export induced upon Cre-mediated deletion of *Ecd* in *Ecd^{fl/fl}* MEFs. GFP expression was used to identify cells infected with control GFP or GFP-Cre adenovirus (green cells). Western blotting confirmed the expression of exogenous FLAG-tagged ECD, ECD-P617G mutant, or DDX39A versus that of the vector-alone transduced cells (Fig. 4A). RNA FISH analysis for poly(A) mRNA showed the expected nuclear accumulation of poly(A) mRNA in GFP-Cre-infected cells transduced with vector alone (Fig. 4B, row 2 versus row 1). Notably, MEFs with *Ecd* deletion that were transduced with human ECD showed nuclear/cytoplasmic poly(A) mRNA signals comparable to those without *Ecd* deletion (seen as red dots in the cytoplasm) (Fig. 4B, compare rows 5 and 6), indicating rescue of the mRNA export block. In contrast, *Ecd*-deleted MEFs transduced with ECD-P617G mutant did not show a rescue of the poly(A) mRNA export block induced by *Ecd* deletion (Fig. 4B, compare rows 7 and 8). Notably, expression of exogenous DDX39A expression did not rescue the mRNA export block induced by *Ecd* deletion (Fig. 4B, compare rows 3 and 4), indicating that ECD may function downstream of DDX39A in mRNA export. Quantification of nuclear/cytoplasmic mRNA signals normalized to $-\text{Cre}$ and vector alone confirmed rescue of *Ecd* deletion-induced mRNA export block by ECD but not by ECD-P617G mutant or DDX39A (Fig. 4C). Taken together, these results demonstrate that interaction of ECD with DDX39A is required for its role in mRNA export and that ECD plays a distinct role that cannot be fulfilled by DDX39A itself.

Given our previous findings that ECD protein is overexpressed in cancers (38, 39), including breast cancers (BC), we wished to analyze if overexpression of ECD protein is due to increased mRNA levels and if mRNA export function of ECD relates to its oncogenic function in breast cancer cells.

ECD mRNA is overexpressed in breast cancer patients, and its mRNA overexpression serves as an independent prognostic marker that predicts survival in breast cancer patients. Analyses of two publicly available data sets, METABRIC (expression based on microarray) and TCGA (expression based on transcriptome sequencing [RNA-seq]), showed that ECD is overexpressed in BC tissues compared to that in adjacent normal breast tissue samples, as shown in the TCGA data set (Fig. 5A). When molecular subtypes were considered, ECD overexpression was seen in the estrogen receptor-positive (ER⁺)/progesterone receptor-positive (PR⁺) (luminal class) and HER2⁺ BC subtypes (Fig. 5B and C). Survival analysis showed that ECD overexpression significantly correlates with poor BC patient survival in the whole cohorts as well as in the hormone receptor-negative, TNBC, and HER2⁺ subgroups (Fig. 5D to K), supporting and confirming our previous immunohistochemistry (IHC) analysis. In addition, higher ECD expression was associated with variables characteristic of poor prognosis, including lymphovascular invasion (LVI) ($\chi^2 = 8.150$, $P = 0.004$) and higher Nottingham prognostic index (NPI) scores, and with the luminal B subtype and the integrative clusters 5 and 6 (see Table S2A). To further evaluate the prognostic importance of *ECD* mRNA expression, we performed multivariate analyses with a model incorporating clinical features (age, tumor size, tumor grade, ER status, PR status, and HER2 status) in both TCGA and METABRIC cohorts, and *ECD* overexpression was shown to be an independent significant predictor of poor outcome (see Table S2B).

To examine whether there is a concordance between ECD mRNA and its protein expression, we assessed the correlation of ECD protein and mRNA expression, which shows a statistically significant positive linear association between ECD protein and mRNA expressions ($r = 0.21$, $P = 0.011$).

FIG 3 Legend (Continued)

(A and D) WB shows ECD or DDX39A KD. (B and E) Cells were fixed and hybridized with 12 μM oligo(dT) 22-nt Quasar 570 probe and then imaged using a LSM 710 Zeiss confocal microscope at $\times 63$ magnification. Last column shows enlarged view of cells shown in the insets. (C and F) Quantification of nucleus-to-cytoplasmic signal ratio (N/C) was conducted using ImageJ software in at least 100 cells, and graphs were plotted by normalizing to the control cells to calculate the fold change. (G to I) *ECD^{fl/fl}* cells were either treated with GFP (control) or Cre-GFP adenovirus to delete ECD. (G) WB shows Cre-mediated knockdown of ECD; β -actin was used as a loading control. (H) Cells were fixed and imaged as discussed above. (I) Quantifications of at least 25 cells using ImageJ to measure nucleus-to-cytoplasmic signal ratio (N/C) by normalizing to the control cells to calculate the fold change. Significance of the ratios was calculated using Student's two-tailed *t* test; *, $P \leq 0.05$, error bars represent standard errors from the mean (SEs). Means \pm SEs were derived from three different experiments. Bars, 10 μm .

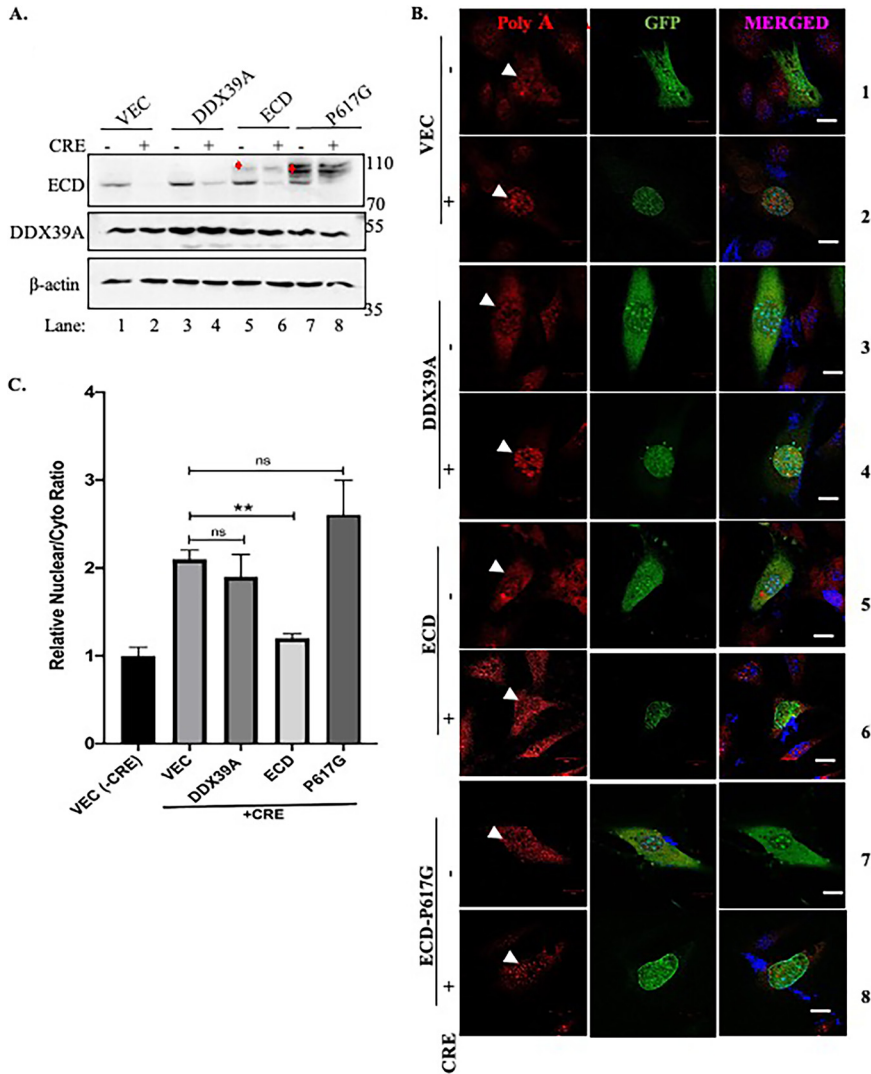


FIG 4 ECD interaction with DDX39A is required for mRNA export. RNA FISH analysis was performed on *Ecd^{fl/fl}* MEFs overexpressing either vector, ECD, DDX39A, or ECD-P617G after treatment with GFP (control) or Cre-GFP adenovirus to delete ECD. (A) WB shows Cre-mediated knockdown of ECD. Exogenous ECD indicated by red marks. β -Actin was used as a loading control. (B) Cells were fixed and hybridized with 12 μ M oligo(dT) 22-nt Quasar 570 probe and then imaged at $\times 63$ magnification. Bars, 10 μ m. (C) Quantifications of nucleus-to-cytoplasmic signal ratios were conducted using ImageJ software in at least 75 cells, and graphs were plotted by normalizing to the control cells. Significance of the ratios was calculated using Student's two-tailed *t* test between groups as indicated, error bars represent standard errors from the means. *, $P \leq 0.05$; **, $P \leq 0.01$; ***, $P \leq 0.001$.

Taken together, these analyses in two independent BC data sets affirm that ECD mRNA overexpression is associated with adverse prognostic features and shorter survival of patients.

ECD regulates ErbB2 mRNA export and stability. As the driver oncogene, ErbB2 mRNA biogenesis is pivotal for oncogenesis (53); thus, we wished to examine if ECD plays a role in ErbB2 mRNA export. First, we transfected ErbB2-overexpressing SKBR3 and BT-474 or epidermal growth factor receptor (EGFR)-overexpressing MDA-MB-468 BC cell lines with control or two independent ECD siRNAs and then examined the levels of ErbB2 and EGFR. ECD KD in both ErbB2-overexpressing cell lines (SKBR3 and BT-474), as well as in MDA-MB-468 (does not overexpress ErbB2), resulted in a reduction in ErbB2 protein levels (Fig. 6A). On the other hand, there was no change in EGFR protein levels in either the EGFR-overexpressing MDA-MB-468 cells or in other two cell

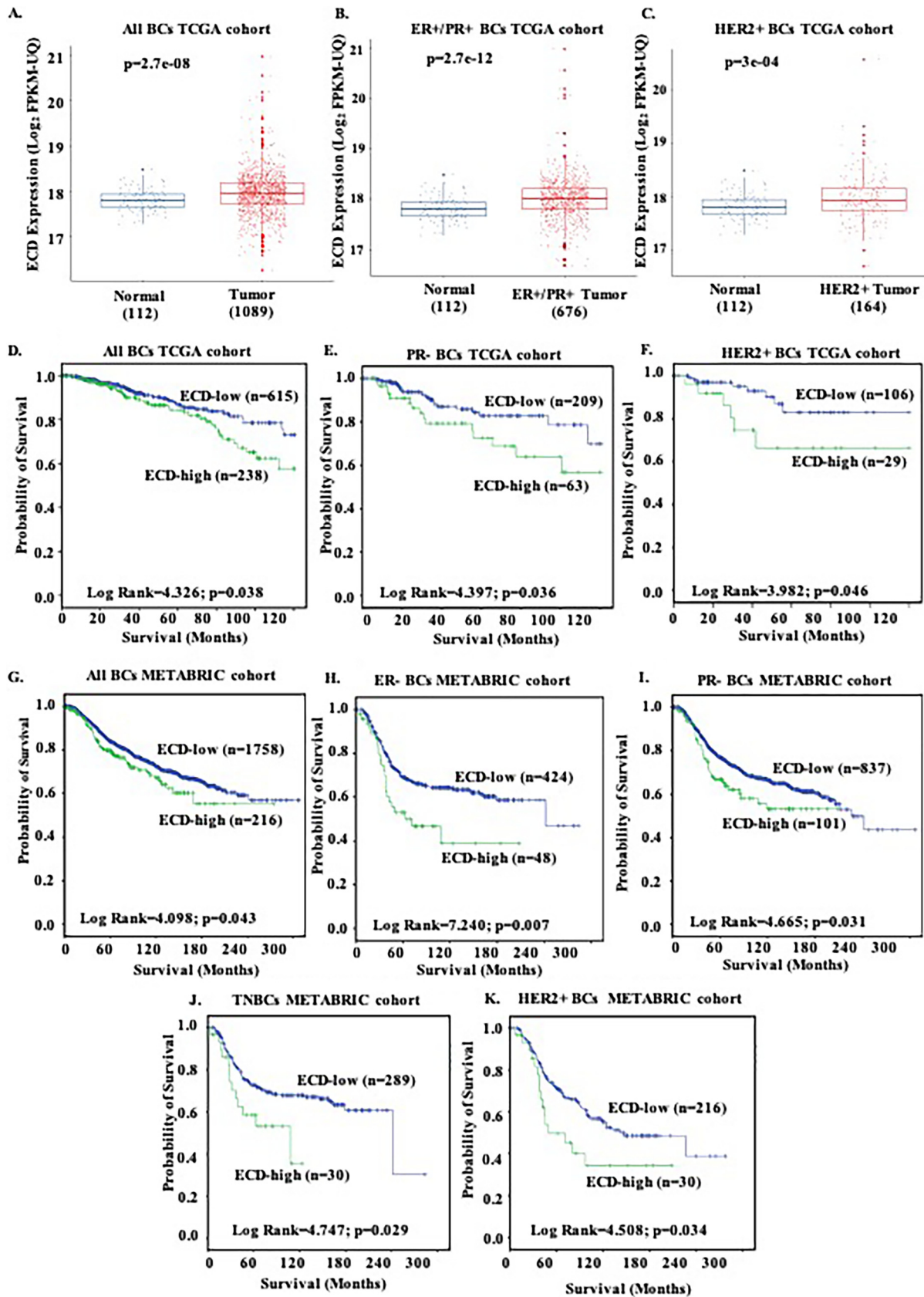


FIG 5 ECD mRNA analyses in breast cancer The Cancer Genome Atlas (TCGA) and the Molecular Taxonomy of Breast Cancer International Consortium (METABRIC) data sets reveal ECD mRNA overexpression correlates with poor patient survival. (A) TCGA breast cancer data set (Continued on next page)

lines that express lower basal EGFR levels (Fig. 6A). Notably, analyses of ErbB2 and EGFR mRNA levels using quantitative real-time PCR (qRT-PCR) showed that ECD KD resulted in a drastic reduction in ErbB2 mRNA levels (Fig. 6B). *DHFR*, an E2F target gene whose expression we have previously shown to be reduced in *Ecd* knockout MEFs (31), served as a positive control. Compared to a marked reduction in ErbB2 mRNA levels, no reduction was observed in EGFR mRNA levels upon ECD KD (Fig. 6B).

Next, we assessed if ECD is transcriptionally regulating ErbB2 by overexpressing exogenous ErbB2 under the cytomegalovirus (CMV) promoter in MCF-7 cells (express low levels of endogenous ErbB2). Vector- or ErbB2-expressing MCF-7 cells were treated with control siRNA or ECD siRNA, followed by analyses of RNA by qRT-PCR and protein by Western blotting. Significant decreases in ErbB2 mRNA and protein levels were observed upon ECD KD (Fig. 6C and D), excluding the transcriptional regulation of ErbB2 by ECD.

In addition, we examined if the decrease in ErbB2 mRNA levels upon ECD KD is due to decreased mRNA stability. For this purpose, two breast cancer cell lines, SKBR3 and BT-474, were treated with actinomycin D, a transcriptional blocker agent, after ECD KD. Total RNA was isolated at designated time points after actinomycin D treatment. qRT-PCR was performed to analyze ErbB2 mRNA levels. In ECD-downregulated cells, at zero time point, the ErbB2 mRNA levels were low compared to those in control cells. As time progressed, the mRNA in control cells was more stable. Notably, the ErbB2 mRNA half-life was approximately 7 to 8 h in scrambled siRNA-expressing SKBR3 and BT-474 cells, similar to previously published data (54, 55). However, ECD KD reduced the ErbB2 mRNA stability to approximately 2 to 3 h (Fig. 6E and F).

Previous studies showed ECD interacts with PRPF8 and has been identified as part of spliceosome complex; therefore, we assessed if ECD KD affects ErbB2 splice variants. We examined the expression of two well-documented splice variants, herstatin (generated by inclusion of intron 8) and Δ 16HER2 (produced due to skipping of exon 16) (56–58). Notably, ECD KD resulted in alterations in the mRNA levels of both splice variants (Fig. 6G). Significantly, ECD KD led to an increase in the expression of herstatin, a tumor suppressor splice variant (58–60), but a reduction in the expression of the Δ 16HER2 variant, a prooncogenic splice variant (57, 61, 62). Taken together, we demonstrate transcriptional regulation of ErbB2 and its splice variants by ECD.

Next, we examined the effect of DDX39A KD on the levels of ErbB2 mRNA and protein. We observed similar decreases in ErbB2 protein (Fig. 7A) and mRNA (Fig. 7B) levels upon DDX39A KD as well as ECD KD. To assess if the decrease in ErbB2 mRNA levels upon ECD KD or DDX39A KD was due to a block in ErbB2 nuclear export, we quantified ErbB2 mRNA levels in nuclear versus cytoplasmic fractions of control versus ECD or DDX39A KD cells. The qRT-PCR analyses revealed a higher nuclear-to-cytoplasmic ratio of ErbB2 mRNA in ECD or DDX39A KD cells than in controls in SKBR3 (Fig. 7B and C) and in BT-474 (Fig. 7D and E) cells; supporting the conclusion that KD of ECD or DDX39A reduces the export of ErbB2 mRNA from the nucleus to the cytoplasm. The purity of nuclear and cytoplasmic fractions was confirmed by analyzing the long non-coding RNA MALAT1 (Fig. 7F) and 18s rRNA and U1 snRNA (Fig. 7G) (63).

Next, we performed ErbB2 mRNA FISH analysis using an ErbB2-specific RNA probe using SKBR3 cells. Consistent with the ECD requirement for ErbB2 mRNA export, the ECD KD cells showed an accumulation of ErbB2 mRNA in the nucleus (more red dots in

FIG 5 Legend (Continued)

comprising a total of 1,089 breast cancer cases, including 676 cases of ER⁺/PR⁺, 164 cases of HER2⁺, and 112 adjacent normal tissue samples, was analyzed for ECD mRNA expression. RNA-seq expression level read counts were normalized using the upper quartile fragments per kilobase to transcript per million mapped reads (FPKM-UQ) calculation, and ECD expression in box plots is represented as log base 2 compared to that in adjacent normal tissue. In TCGA cohorts, ECD mRNA expression is significantly higher in all breast cancer tissues than in adjacent normal breast tissues ($P = 2.7e-08$) (A), in ER⁺/PR⁺ breast cancer samples ($P = 2.7e-12$) (B), and in HER2⁺ breast cancer cases ($P = 3e-04$) (C). (D) The 10-year overall survival of 854 cases was significantly worse in ECD-high (238) than in ECD-low (616) mRNA-expressing patients. High ECD mRNA expression in PR⁻ subgroup (E) and HER2⁺ (F) subgroup of TCGA data set correlates with poor survival. (G) METABRIC cohort: Kaplan-Meier plot for survival curve of all the breast cancer patients shows poor prognosis with high ECD mRNA, including in the ER⁻ subgroup (H), PR⁻ subgroup (I), triple-negative breast cancer (TNBC) subgroup (J), and HER2⁺ subgroup (K). Cox regression analysis results are shown with the Kaplan-Meier plots.

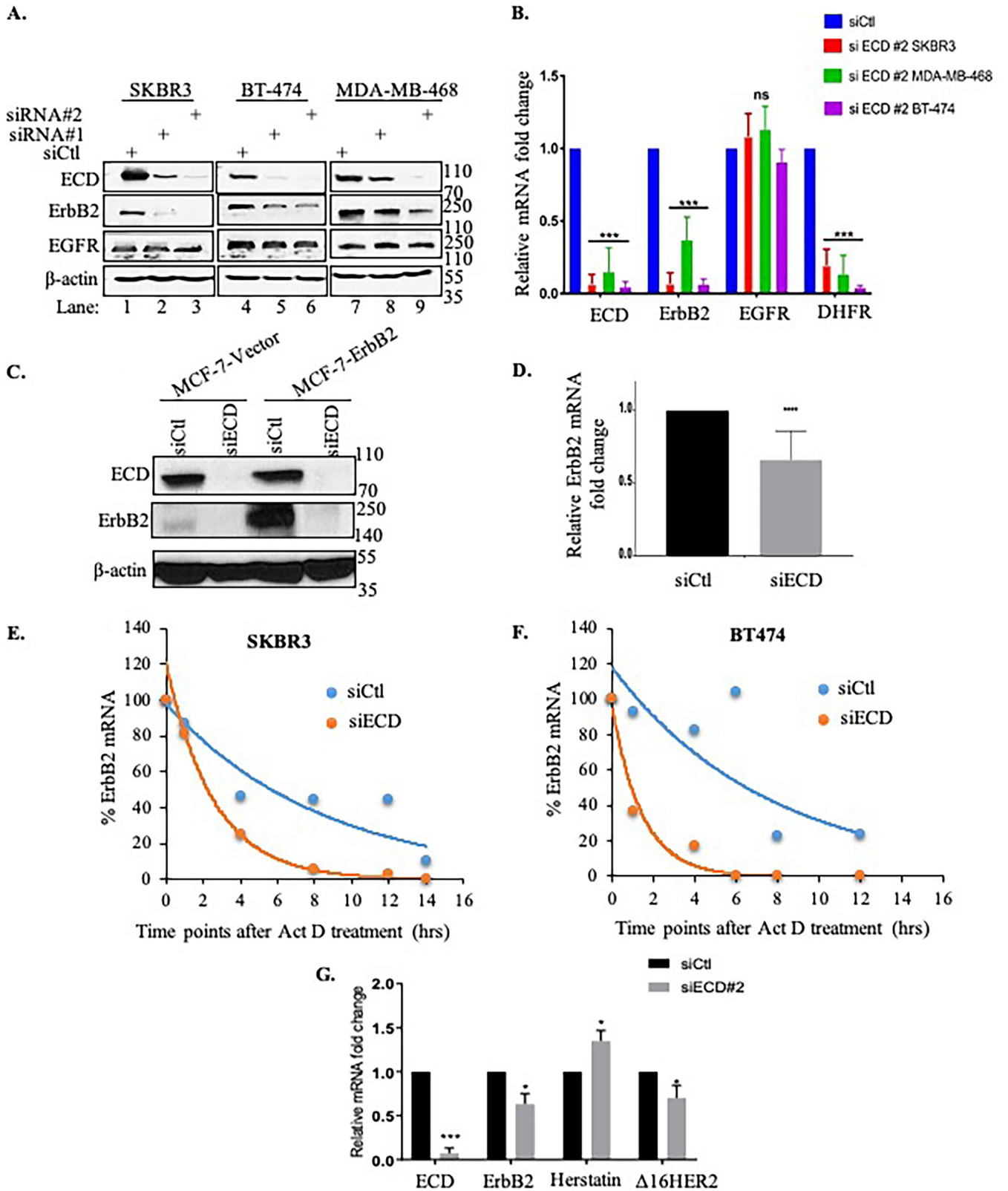


FIG 6 ECD KD decreases ErbB2 protein and mRNA expression in breast cancer cells. ECD knockdown was performed using specific siRNA against ECD in BT-474, SKBR3 (ErbB2-overexpressing), and MDA-MB-468 (EGFR-overexpressing) breast cancer cell lines. Protein and total mRNA were isolated after 48 h of transfection. (A) Lysates were harvested and immunoblotted with the indicated antibodies. β-Actin was used as a loading control. (B) Control mRNA levels of ECD, ErbB2, or EGFR were detected by qRT-PCR; DHFR was used as a positive control, and GAPDH served as an internal control. Fold change over GAPDH was calculated and plotted and normalized with control. (C) MCF-7-vector and MCF-7-ErbB2 expressing cells were treated with ECD siRNA or

(Continued on next page)

the nucleus) (Fig. 7H). Quantification of the nuclear versus cytoplasmic ErbB2 mRNA signals showed a higher nuclear/cytoplasmic ratio of ErbB2 mRNA signals upon ECD KD (Fig. 7I).

Taken together, these experiments demonstrate that ECD is an essential protein required for ErbB2 mRNA processing from the nucleus to the cytoplasm.

Requirement of ECD for oncogenic traits of ErbB2-overexpressing breast cancer cells. ECD protein is overexpressed in a significant subset of breast cancers and is also upregulated in other cancers (38–41), and its overexpression correlates with poor prognosis and short survival in ErbB2-overexpressing breast cancers (39). Thus, our findings that ECD is required for the nuclear export of the mRNA for this driver oncogene and to maintain high ErbB2 mRNA and protein levels in ErbB2-overexpressing breast cancer cells suggested the strong likelihood that ECD would be required for ErbB2-driven oncogenic traits. We therefore assessed the functional consequences of ECD KD on key *in vitro* oncogenic traits of ErbB2-overexpressing breast cancer cell lines. ECD KD in BT-474 and SKBR3 cell lines (Fig. 8A) significantly decreased cell proliferation (Fig. 8B and C) (significant at days 6, 8, and 10), colony formation (Fig. 8D, E, and F) (measured after 10 days of seeding), and anchorage-independent growth as measured by the soft agar colony growth assay (Fig. 8G and H) (measured 21 day after seeding). In addition, ECD KD cells exhibited a significant decrease in their ability to migrate across Transwell chambers (Fig. 9B) and to invade through Matrigel (Fig. 9C). Taken together, these results demonstrate that ECD is needed for ErbB2 mRNA export and that optimal expression translates into a requirement of ECD for ErbB2-driven oncogenesis.

DISCUSSION

In this study, we provide evidence that ecdysoneless (ECD), a protein evolutionarily conserved from yeast to humans, is required for export of mRNAs from the nucleus to the cytoplasm through its interaction with DDX39A. Consequently, ECD KD in ErbB2⁺ breast cancer cells led to decreases in ErbB2 mRNA levels and its stability, which was associated with impairment of oncogenic traits.

First, using mass spectrometry analyses of affinity-purified ECD, we identified a number of ECD-associated proteins known to be involved in mRNA processing, including mRNA export (see Table S1A and B in the supplemental material). The ECD-associated proteins included DDX39A, a known mRNA export regulatory protein. We confirmed the interaction of ECD with DDX39A, using immunoprecipitation followed by Western blotting, immunofluorescence colocalization, and GST fusion protein pull-down experiments. ECD truncation mutational analyses suggested that the middle part of ECD (amino acids 150 to 438) is where ECD interacts with DDX39A (Fig. 1G). However, further detailed mutational analyses will be needed to more precisely localize the region/motif within ECD that interacts with DDX39A. Notably, a single amino acid change (ECD-P617G), modeled after a *Drosophila ecd* mutant previously shown to cause molting defects (50), lacked the ability to interact with DDX39A even though the mutation is not within the DDX39A-interacting region of ECD. Since this mutant retained the ability, like wild-type ECD, to associate with the RUVBL1 component of the R2TP complex (Fig. 1G), it is unlikely that the lack of association with DDX39A is due to misfolding of this protein, although structural studies will be needed to rule

FIG 6 Legend (Continued)

control siRNA, and lysates were collected and blotted with indicated antibodies. (D) RNA was isolated, cDNA was prepared, and qRT-PCR was performed using ErbB2-specific primers. Fold change with respect to control after normalizing with β -actin was calculated and plotted. ECD downregulation decreases ErbB2 mRNA stability. (E and F) The stability of mRNA was analyzed in SKBR3 and BT-474 breast cancer cell lines. After ECD downregulation by siRNA, cells were treated with actinomycin D (5 μ g/ml) at zero time point, and then total RNA was isolated at various time points (0, 2, 4, 6, 8 and 12 h) after actinomycin D treatment. cDNA was made, and levels of ErbB2 were measured by qRT-PCR. GAPDH was used as normalization control. (G) qRT-PCR using specific primers of indicated genes from RNA samples of SKBR3 cells treated with control and ECD siRNA. ECD knockdown was confirmed. HER2 (full form) and its isoforms, herstatin and Δ 16HER2, were analyzed using specific sets of primers. β -Actin was used as an internal control. Fold change with respect to control after normalizing with β -actin was calculated and plotted. Significance of the ratios was calculated using Student's two-tailed *t* test. ns, not significant; *, $P \leq 0.05$; **, $P \leq 0.01$; ***, $P \leq 0.001$. Error bars represent means \pm standard deviations (SDs) from six replicates in a representative experiment. The experiment was repeated three times independently.

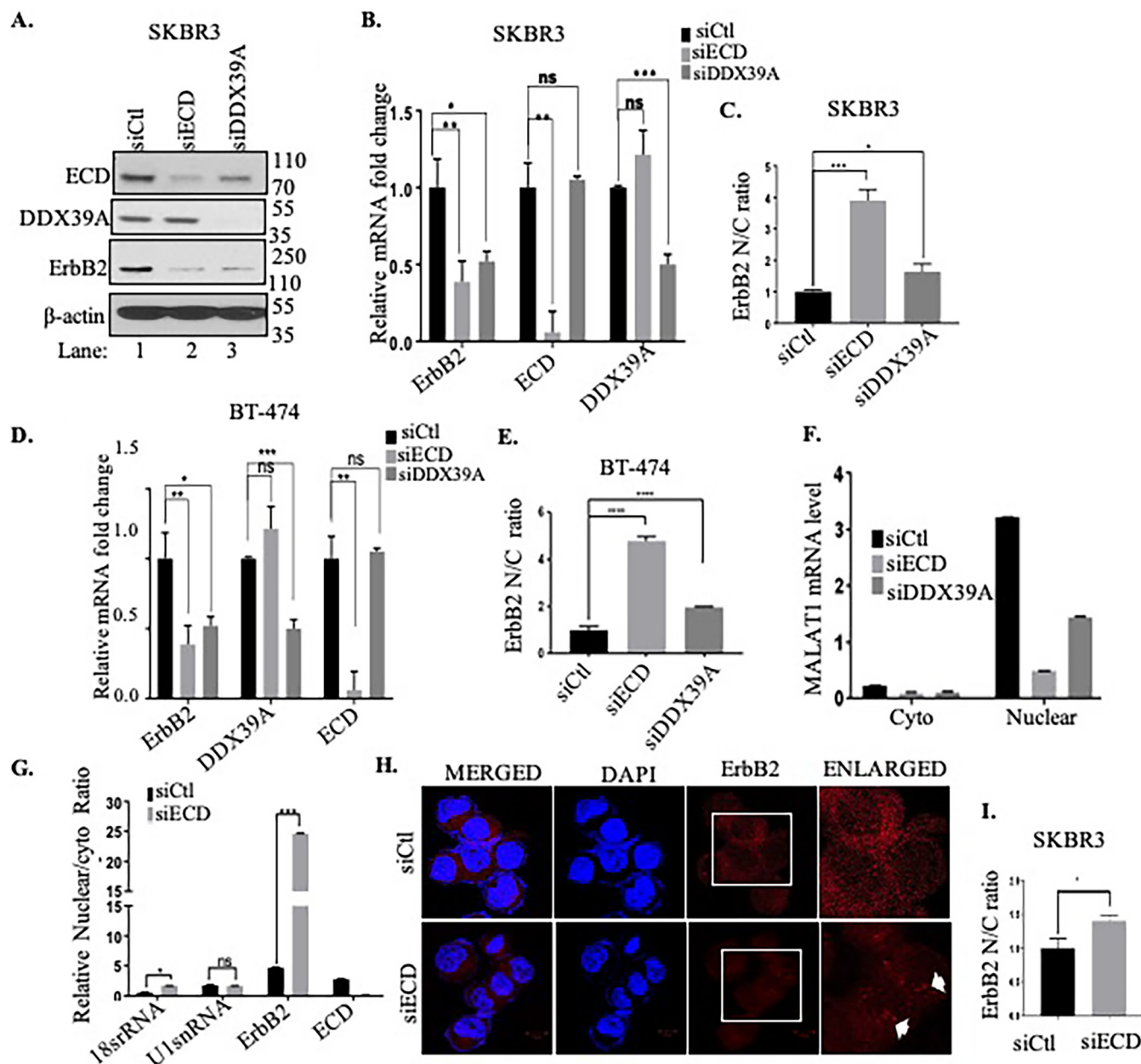


FIG 7 ECD KD increases nuclear ErbB2 mRNA accumulation. SKBR3 and BT-474 cells were transfected with control siRNA, ECD siRNA, and DDX39A siRNA. (A) Western blotting was performed with indicated antibodies; β -actin was used as a loading control, confirming knockdown of ECD and DDX39A in SKBR3. (B and D) qRT-PCR shows decrease in ErbB2 mRNA in ECD or DDX39A KD cells in comparison to control siRNA-treated cells. The graph plotted shows ECD, ErbB2 and DDX39A mRNA levels normalized to β -actin, and fold change was calculated by normalizing to control in SKBR3 (B) and in BT-474 (D) cells. SKBR3 cells were subjected to subcellular RNA fractionation after treating the cells with control siRNA, ECD siRNA, and DDX39A siRNA. (C and E) Subcellular RNA fractionation after control siRNA, ECD siRNA, or DDX39A siRNA treatment followed by qRT-PCR of ErbB2 mRNA showing nuclear/cytoplasmic ratio (N/C) in SKBR3 (C) and BT-474 (E) cells. (F) qRT-PCR of MALAT1 (a long noncoding RNA) used as control for purification of nuclear fraction. (G) qRT-PCR showing nucleus-to-cytoplasmic ratio of 18S rRNA, U1 snRNA, and ErbB2 and ECD mRNA in control siRNA- and ECD siRNA-treated cells; each cytoplasmic and nuclear fraction was normalized to corresponding total fraction. Significance was calculated using Student's two-tailed *t* test. *, $P \leq 0.05$; **, $P \leq 0.01$; ***, $P \leq 0.001$; ns, nonsignificant, error bars represent standard errors from the means. Means \pm SEs were derived from three different experiments. ECD knockdown was performed using specific siRNA against ECD in SKBR3 cells. (H) RNA FISH analysis was carried out with 12 μ M oligonucleotide anti-ErbB2 570 probe and then imaged at $\times 63$ magnification; last column shows enlarged view of cells. White arrows show the accumulation of ErbB2 mRNA probe. (I) Quantifications of at least 25 cells using ImageJ showing nucleus-to-cytoplasmic ratio (N/C) by normalizing to the control cells to calculate the fold change. Significance of the ratios was calculated using Student's two-tailed *t* test. *, $P \leq 0.05$, error bars represent standard errors from the means. Means \pm SEs were derived from three different experiments.

this out definitively. It is possible that the conformation adopted by the C-terminal region of ECD impacts the ability of N-terminal sequences to engage in protein-protein interactions. Notably, our previous analyses using SAXS revealed that the first 400 residues of ECD form a globular structure, while the adjacent ~ 100 residues were in an

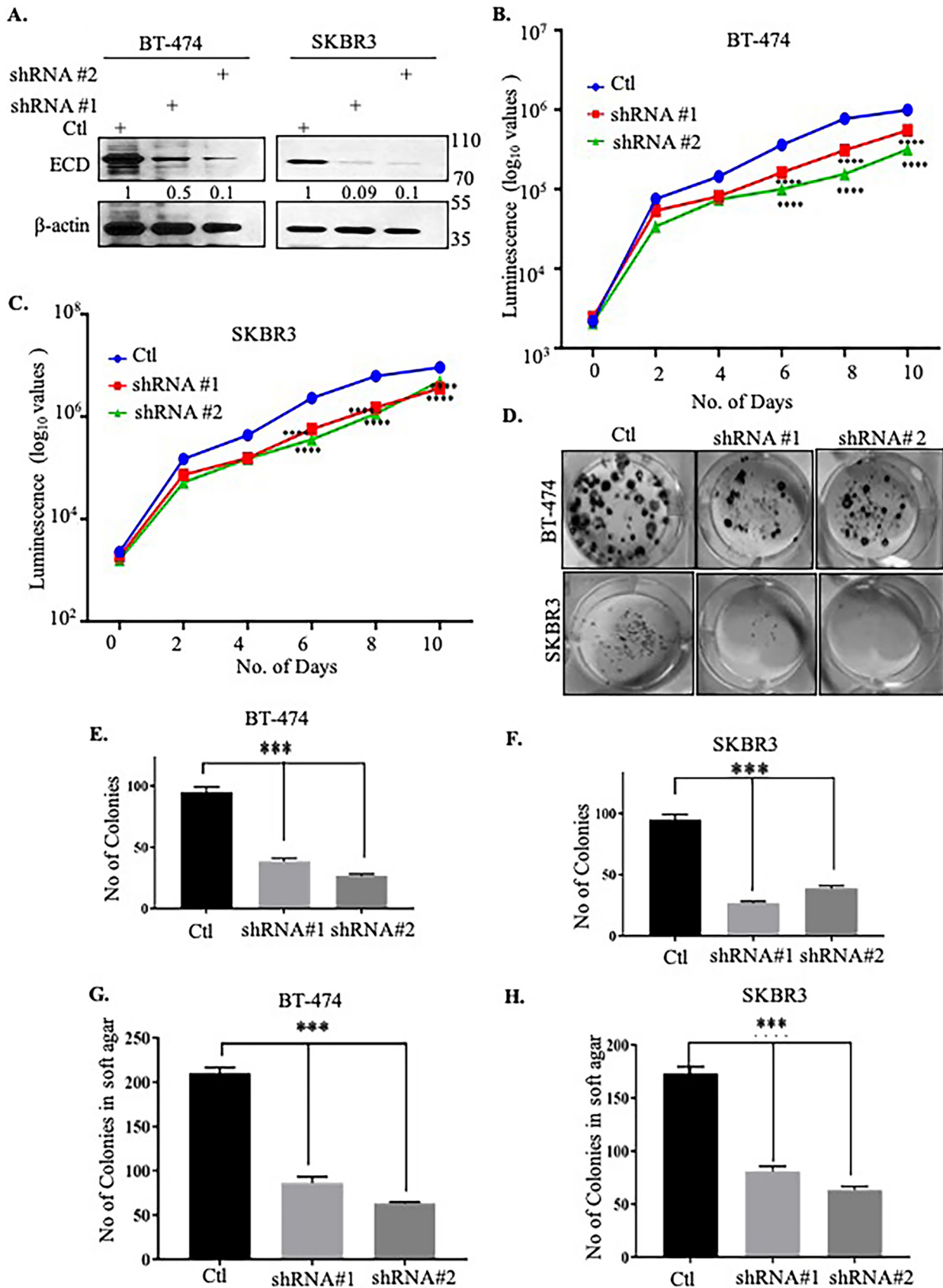


FIG 8 ECD knockdown decreases cell proliferation and anchorage independent of ErbB2-overexpressing breast cancer cells. (A) ECD was stably knockdown by two different shRNAs against ECD, and then KD was assessed by Western blotting. (B and C) Cell proliferation assays were (Continued on next page)

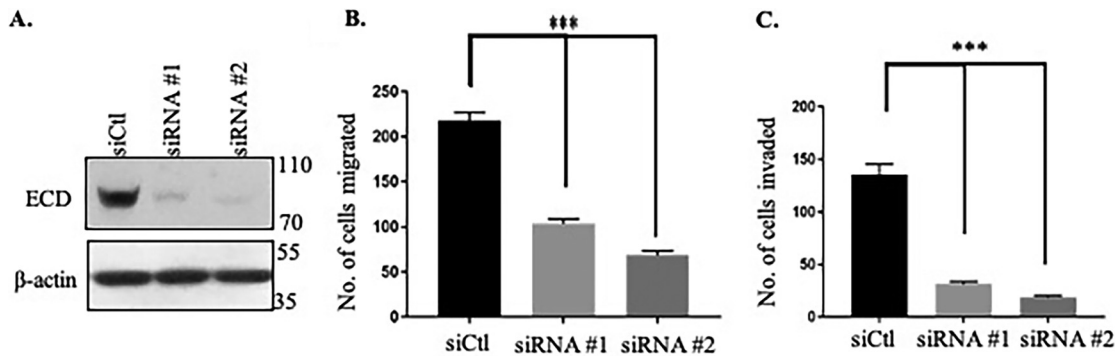


FIG 9 Knockdown of ECD decreases invasion and migration ability of breast cancer cells. BT-474, an ErbB2-positive breast cancer cell line, was treated with control or two independent siRNAs against ECD. (A) Western blotting shows knockdown of ECD with two independent siRNAs. (B and C) Ten thousand cells were counted and plated on Boyden chambers for assessing their ability to migrate (B) and invade (C). After 24 h, cells that had invaded through Matrigel (for invasion assay) and migrated to the bottom surface were fixed and stained with propidium iodide. Pictures were taken, cells were counted, and histograms were plotted. The bar diagrams represent numbers of cells migrated or invaded. ANOVA indicated that the mean number of cells migrated for the control group was higher than those for both ECD siRNA no. 1 and ECD siRNA no. 2 (all Tukey's adjusted P values less than 0.001). *, $P \leq 0.05$; **, $P \leq 0.01$; ***, $P \leq 0.001$; ns, nonsignificant. Means \pm SEs were derived from three different experiments, each performed in triplicates.

extended cylindrical conformation (33), suggesting ECD may function as a scaffolding protein. These structural features suggesting the flexibility of the C-terminal region and the more compact structure in the area where DDX39A interacts are consistent with the potential interactions between N- and C-terminal regions of ECD affecting its interactions, in this case, with DDX39A. Consistent with this possibility, ECD interaction with RUVBL1 involves the more proximal N-terminal sequences (1 to 155) that are dispensable for DDX39A interaction (Fig. 1G).

The multipronged analyses discussed above revealed that ECD exists as a part of protein complexes previously implicated in mRNA export. Multiple approaches supported this prediction: ECD depletion and mRNA export using FISH analyses of poly(A) mRNA (Fig. 3) and biochemical fractionations of nuclear and cytoplasmic mRNA (Fig. 7) showed that ECD is required for mRNA nuclear export. Use of siRNA-mediated ECD KD, inducible ECD KD in human cell lines, and adenovirus-Cre mediated *Ecd* knockout in *Ecd*^{fl/fl} MEFs provided complementary approaches to lend strong support for a requirement of ECD in mRNA export. Furthermore, restoration of blocked mRNA export in *Ecd*^{fl/fl} MEFs subjected to Cre-mediated *Ecd* deletion by reexpressing exogenous human ECD (Fig. 4) strengthened the conclusion that ECD is critical in mRNA export. Notably, overexpressing exogenous DDX39A in *Ecd*-deleted MEFs did not restore mRNA export, suggesting that ECD may also interact with other proteins involved in the mRNA export process. Consistent with this possibility, we observed ECD interaction with several RNA processing proteins, including DDX39B (Table S1A and B). However, interaction with DDX39A appears to be important for ECD's role in mRNA export, as the ECD-

FIG 8 Legend (Continued)

performed using CellTiter-Glo luminescent cell viability assay; 2,000 cells per well were plated (as discussed in Materials and Methods). Readings were taken at the indicated days and \log_{10} transformed to meet ANOVA assumptions. Graphs were plotted based on the mean of \log_{10} -transformed readings for each group at each time point. The corresponding standard errors were very small and not plotted. ANOVA indicated that mean \log_{10} -transformed readings of the control group were higher than those of both ECD shRNA no. 1 and ECD shRNA no. 2 at days 6, 8, and 10 (all Tukey's adjusted P values less than 0.0001). (D) For colony formation assay, 10,000 cells were plated in 6-well plate, and colonies were fixed and then stained with crystal violet after 10 days of plating. (E and F) Colonies were counted and presented as histograms for BT-474 (E) and SKBR3 (F) cells. ANOVA indicated that the mean number of colonies of the control group was higher than those of both ECD shRNA no. 1 and ECD shRNA no. 2 (all Tukey's adjusted P values less than 0.001). (G and H) Soft agar colony formation assay was used to measure anchorage dependence; 20,000 cells were plated in 0.3% agarose in 6-well plates for 21 days (described in detail in Materials and Methods), and then colonies were stained with 0.05% crystal violet. Colonies were counted and plotted as histograms for BT-474 (G) and SKBR3 (H) cells. ANOVA indicated that the mean number of colonies of control in soft agar was higher than those of both ECD shRNA no. 1 and ECD shRNA no. 2 (all Tukey-adjusted P values less than 0.001). *, $P \leq 0.05$; **, $P \leq 0.01$; ***, $P \leq 0.001$; ns, nonsignificant. Means \pm SEs were derived from three different experiments, each performed in triplicates.

P617G mutant, which did not associate with DDX39A (Fig. 1G), was unable to rescue the block in mRNA export in *Ecd*-deleted MEFs (Fig. 4A and B). Our results are consistent with the impact of ECD-associated protein REF/ALY depletion, which results in mRNAs in the nucleus (64, 65). Given the association of ECD with CRM1 and ALY, future studies are warranted to assess the potential CRM1-dependent versus -independent roles of ECD in mRNA export (24, 66).

Using genetic knockout studies, we have previously shown a physiological role of ECD in embryogenesis, cell cycle regulation, and cell survival (31, 32, 37) and *Drosophila Ecd* is also critical in embryonic development and cell survival (50). To what extent the role of ECD in mRNA export is important in its physiological functions remains conjectural at present and will require further structural and mutational information that might selectively eliminate its mRNA export versus other functions, such as its role in mitigating endoplasmic reticulum stress (32), roles mediated through interactions with the R2TP complex, and others. In the context of mRNA processing itself, which involves integrated events, including transcription, capping, splicing, and transport, and other processing events to allow the availability of translation-ready mRNA in the cytoplasm (4–6, 67), it will be of considerable interest to determine to what extent the new role of ECD in mRNA export we describe here is linked to or distinct from its PRPF8-dependent role in mRNA splicing (30). ECD's previously established interaction with the PIH1D1 and RUVBL1 components of the R2TP cochaperone complex (37) may allow it to play an even broader role in RNA biogenesis. The R2TP complex is known to promote the assembly of small nucleolar ribonucleoproteins (snoRNPs) (34, 35, 68–73). Notably, ECD was also reported to interact with ZINHIT2 protein, which was shown to function as a mediator of R2TP/prefoldin-like cochaperone interaction with the U5 snRNP (34, 72), a central component of the spliceosome (35). Thus, the ECD-R2TP complex could play a role in promoting mRNA splicing. Our present studies link ECD with multiple mRNA processing proteins involved from splicing to translation of mRNA, and future studies will help decipher a potential role for the ECD-R2TP interaction in mRNA export, splicing, and possibly other aspects of RNA biogenesis.

ECD protein is overexpressed in multiple cancers (38, 39, 41). As heightened metabolic, migratory, proliferative, and other requirements of cancer cells require increased demand on mRNA processing for both driver oncoproteins and general biochemical pathways (74–81), one mechanism by which overexpressed ECD may contribute to oncogenic drive is to ensure efficient mRNA export that is linked to aid and enable oncogenesis (81). In breast cancer, ECD protein is overexpressed and its overexpression is correlated with shorter survival, particularly in ErbB2-overexpressing patients (39). However, it remained unclear if the ECD protein overexpression was related to increase mRNA expression. Using publicly available TCGA and METABRIC data sets, we demonstrate *ECD* mRNA is overexpressed in BC and its overexpression predicted shorter survival in ER⁻, PR⁻, and TNBC as well as HER2⁺ BC subtypes (Fig. 5). Association of higher *ECD* mRNA expression with lymphovascular invasion (LVI), NPI group 3, and lymph node stage 3 (Table S2A) and the ability to independently predict poorer patient outcomes (Table S2B) supported a potentially important role of ECD in BC tumorigenesis. Importantly, our findings that ECD overexpression in BC reflects increased mRNA levels provided a strong rationale to mechanistically examine how ECD regulates ErbB2 mRNA.

As ErbB2 overexpression in most breast cancer patients represents increased transcription from an amplified *ErbB2* gene locus (82), the oncogenic drive is likely to depend on efficient processing of the mRNA for the driver oncogene ErbB2. Our analyses demonstrate that ECD is indeed critical for ErbB2 mRNA export. ECD KD markedly reduced the levels of ErbB2 mRNA but not the levels of EGFR mRNA, even in a cancer cell line with EGFR overexpression (Fig. 6B). FISH analyses confirmed the requirement of ECD for ErbB2 mRNA nuclear export (Fig. 7H and I). Analysis of mRNA levels in cytoplasmic and nuclear fractions further demonstrated the requirement of ECD for ErbB2

mRNA export (Fig. 7A to G). Similar results were observed upon DDX39A KD (Fig. 7A to G). The marked reduction in ErbB2 mRNA levels upon ECD KD reflected destabilization of ErbB2 mRNA secondary to its nuclear retention (Fig. 6E and F), as nuclear export block is known to trigger degradation of certain mRNAs (83). Notably, ECD KD also decreased the levels of exogenously overexpressed ErbB2 (Fig. 6C and D), thus eliminating the possibility of transcriptional regulation of ErbB2 expression by ECD.

Notably, not only full-length ErbB2 but also ECD KD altered the expression levels of two ErbB2 splice variants. One splice variant, $\Delta 16\text{HER2}$, is known to be highly tumorigenic compared to other isoforms and has been associated with increased invasive and metastatic properties and even trastuzumab resistance (84). ECD KD reduces the level of the $\Delta 16\text{HER2}$ variant and may also be attributable to the decrease in oncogenic potential of ErbB2⁺ cell lines. However, ECD KD resulted in increased levels of herstatin, which acts as a tumor suppressor by effectively blocking HER2 activity and cell proliferation while promoting apoptosis (58, 59), supporting the notion that ECD is an important player in ErbB2-mediated oncogenesis.

ECD-dependent ErbB2 mRNA export is functionally relevant in the context of overexpressed ECD in cancer cells, which is supported by our observations that KD of ECD dramatically reduced the oncogenic traits (Fig. 8 and 9). These results are consistent with our previous results that ECD provides a co-oncogenic function with mutant Ras protein to fully transform the nontumorigenic immortal human mammary epithelial cells (42). Notably, overexpression of DDX39A was reported to regulate growth and metastasis of various cancer types (46, 49, 76–79). Other studies have shown that DDX39A is also required to maintain the genome integrity and telomere protection, processes that are rendered aberrant as cells become cancerous (85–88).

Taken together, our studies reveal a novel role of ECD, an independent prognostic marker in breast cancer patients, as an essential and important component of the mRNA export machinery. Using ErbB2-overexpressing breast cancer cell lines, we implicate ECD as a regulator of ErbB2 mRNA export and stability to promote ErbB2-driven oncogenic traits. Given the importance of ECD in the cell cycle, cell survival, and embryogenesis and its overexpression across human cancers, our findings provide a new mechanism that could help understand the physiological and pathological roles of ECD.

MATERIALS AND METHODS

Biochemical reagents. Formaldehyde solution (F8775), doxycycline (DOX; D9891), puromycin (P8833), Triton X-100 (T9284), and IGEPAL CA-630 (NP-40; I3021) were from Sigma-Aldrich. Hygromycin B (10687010) was purchased from Thermo Fisher Scientific. Anti-FLAG M2 affinity gel (A2220) and FLAG peptide (3 \times FLAG; F4799), Met-Asp-Tyr-Lys-Asp-His-Asp-Gly-Asp-Tyr-Lys-Asp-His-Asp-Ile-Asp-Tyr-Lys-Asp-Asp-Asp-Lys, were from Sigma-Aldrich. Glutathione-Sepharose 4B beads (17-0756-01) and PreScission protease (27-0843-01) were from GE Healthcare.

Antibodies. The mouse monoclonal antibody against ECD was previously described (31, 39). The antibodies used in these studies include those against PRPF8 (ab79237), DDX39A (ab96621), LRPPRC (ab97505), and ALY (ab202894) and were from Abcam. Antibodies against CRM1 (46249) and ErbB2 (22425) were purchased from Cell Signaling. For immunofluorescence staining, we used anti-ECD (catalog number HPA006465; Sigma-Aldrich) and anti-DDX39 (catalog no. sc-271395; Santa Cruz Biotechnology) antibodies; secondary antibodies tagged with Alexa Fluor 488 (A32731 and A32723) and Alexa Fluor 568 (A-11011 and A-11031) and anti-FLAG antibody (F3165) were from Sigma-Aldrich.

Cell culture, reagents, and transfections/infections. Immortal human mammary epithelial cell lines (hMECs) MCF10A and 76NERT were cultured in DFCl-1 medium (32, 42). HEK-293T cells (ATCC) were maintained in Dulbecco's modified Eagle's medium (DMEM) supplemented with 10% fetal bovine serum (48). Adenoviruses encoding enhanced green fluorescent protein-Cre (adeno-GFP-Cre) or enhanced green fluorescent protein (adeno-GFP; control) were purchased from the University of Iowa Gene Transfer Vector Core. For ECD knockout studies, previously published *Ecd^{fl/fl}* MEFs were maintained in DMEM supplemented with 10% fetal bovine serum and infected with control or GFP-Cre as described previously (31, 32). For tetracycline (TET)-inducible ECD overexpression, a full-length human ECD cDNA was cloned into the pRev-TRE (Hygro) retroviral vector downstream of the tetracycline response element (TRE). Constructs containing ECD or the empty vector or the pMSCV-rTA construct encoding the reverse tetracycline transactivator were transfected into the Phoenix Amphotropic (AMPHO) packaging cell line using a standard calcium phosphate transfection protocol to generate retroviral supernatants. The pRev-ECD or pRev control retroviruses were cotransduced with pMSCV-rTA virus into MCF10A cells using three serial infections with the retroviral supernatants at 12-h intervals followed by selection with 2 $\mu\text{g}/$

ml puromycin and 3 $\mu\text{g/ml}$ hygromycin for 48 h or until all uninfected cells died. To induce the ECD overexpression, vector- or ECD-overexpressing MCF10A cell lines were cultured with 1 $\mu\text{g/ml}$ of doxycycline (DOX), as published previously (32). SKBR3, BT-474, and MDA-MB-468 breast cancer cell lines were purchased from ATCC (Manassas, VA). SKBR3 and BT-474 cells were cultured in RPMI medium supplemented with 10% fetal bovine serum. MDA-MB-468 breast cancer cell line and mouse embryonic fibroblast cells (MEFs) were cultured in DMEM with 10% serum (89). Mycoplasma contamination was examined by 4',6-diamidino-2-phenylindole (DAPI) staining/fluorescence microscopy. For siRNA-based knockdown, cells were transfected with 30 nM ECD siRNA-1, AAGGCCTAATGAGTCAGATTC-deoxyribosylthymine (dT)dT, ECD siRNA-2, AAGAACCAAGUGGAACCCUGAdTdT, control siRNA (sc-37007), or DDX39A siRNA (sc-77111), which were purchased from Santa Cruz Biotechnology, using the DharmaFECT 1 transfection reagent (T-2001-03; Dharmacon, Pittsburgh, PA).

Generation of ECD shRNA knockdown cell lines. ErbB2-overexpressing breast cancer cell lines, SKBR3 and BT-474, were infected with retroviral supernatants corresponding to two distinct ECD shRNAs or a control shRNA, as described previously (38). Virally transduced cells were selected in 0.5 $\mu\text{g/ml}$ puromycin for 3 days, and the expression of endogenous ECD was assessed in whole-cell lysates using Western blotting with an anti-ECD monoclonal antibody (31, 39, 42).

CellTiter-Glo luminescent cell viability assays. Two thousand cells of SKBR3 or BT-474 cell lines expressing the control or ECD shRNAs were seeded per well in 96-well plates (Thermo Scientific, catalog no. 136101) and cultured with changes of medium on alternate days. At the designated times, viable cells were quantified using the CellTiter-Glo luminescent cell viability assay according to the manufacturer's protocol (Promega).

Colony formation assays. SKBR3 and BT-474 cell lines expressing the control or two distinct ECD shRNAs were plated (10,000 cells per well) in six-well plates for 9 days with changes of medium on alternate days. The cells were then fixed and stained with 0.25% crystal violet (in 25% methanol) and then imaged, as described previously (89). Pictures were taken and colonies were counted manually.

Anchorage-independent growth assays. Twenty thousand cells suspended in RPMI medium containing 0.3% agarose were seeded on top of a bottom layer of 0.6% agarose in 6-well plates, as described previously (89, 90). Each cell line was plated in triplicates, and each experiment was repeated three times. Cultures were fed every 2 days. Twenty-one days after cell seeding, the plates were fixed and stained with 0.05% crystal violet in 25% methanol. Pictures were taken and colonies were counted manually (90).

Transwell migration and invasion assays. For migration assays, BT-474 cells transiently transfected with control or ECD-specific siRNAs (described above) were serum-starved in medium with 0.1% FBS for 24 h, and 10,000 cells were plated in top chambers of BD BioCoat Transwell chambers (catalog no. 354578; BD, San Jose, CA). After 2 h, 10% FBS-containing medium was added to the bottom chambers. Migration was then assessed after 24 h by removing the nonmigrated cells on the top surface of the filters, fixation in ice-cold methanol, and staining with propidium iodide, as previously described (42). The filters were mounted on coverslips, and migrated cells on the bottom surface were observed at $\times 10$ magnification under a rhodamine filter using a LSM 710 confocal microscope. Invasion assays were performed as for the migration assay, except for the use of BD Matrigel invasion chambers (no. 354480; BD).

Immunoprecipitation and immunoblotting. For immunoprecipitations, cell extracts were prepared in Triton lysis buffer (20 mM Tris-HCl [pH 7.5], 200 mM NaCl, 1% Triton X-100, and a protease inhibitor cocktail from Roche), and protein concentration was determined using a bicinchoninic acid assay (Pierce BCA protein assay kit, 23225). One-milligram aliquots of lysate protein was immunoprecipitated with 5 μg of antibodies overnight at 4°C. The immune complexes were captured with protein A/G-agarose (sc-2003; Santa Cruz Biotechnology) for an additional 2 h. Samples were prepared by boiling the beads in 2 \times sample buffer and loaded in SDS-PAGE gels, and the gels were transferred to Immobilon transfer membrane (Millipore; IPVH00010), which was blotted with corresponding antibodies and developed with enhanced chemiluminescence substrate (PerkinElmer; NEL05001EA).

GST pulldown assays. GST fusion proteins of ECD or its mutants were purified from bacterial lysates using glutathione-Sepharose 4B, and GST pulldown experiments were performed as described previously (31, 37).

RNA isolation and quantitative real-time PCR. Total RNA was isolated from control and siRNA-treated SKBR3 and BT-474 cell lines using TRIzol reagent (Invitrogen; cat no. 15596018.) according to the manufacturer's protocol. One microgram RNA was reverse transcribed using SuperScript II reverse transcriptase (Invitrogen, Thermo Fisher Scientific, Waltham, MA) and oligo(dT) primers (18-mer), and aliquots were used for quantitative real-time PCR (qRT-PCR) analyses with specific primer sets (Sigma, St. Louis, MO) listed below. qRT-PCR was carried out in an Applied Biosystems 7500 real-time PCR system using Power SYBR green master mix from Applied Biosystems (Thermo Fisher Scientific). Primers used in this study include the following: *ECD*, ACTTTGAAACACACGAACCTGGCG (forward [F]) and TGATGCAGGTGTGTAGTTCCT (reverse [R]); *DHFR*, TAAACTGCATCGTCTGTGT (F) and AGGTTGTGGTCAATCTCTGGAAA (R); *ErbB2*, AGCCCTGCCCATCAACTG (F) and AATGCCAACACCCGAGA (R); *EGFR*, TGCCATCCAACTGCACCTA (F) and CTGTGTTGAGGGCAATGAG (R); *GAPDH*, GTCATCCATGACAAGTTTGG (F) and TGCCAGTGAGCTTCCCGTTC (R); 18S rRNA, GCTTAATTTGAC TCAACACGGGA (F) and AGCTATCAATCTGTCAATCCTGTC (R); *RNU1* snRNA, ATACCATGATCAGGAAGGTGGTT (F) and CAGTCCCCACTACCACAAATTA (R); *HER2- Δ 16*, CACCCACTCCCCTCTGAC (F) and GCTCCACCACTC CGTTTCCCTG (R); and herstatin, AGCTGTGTGACTGCCTGTCCCT (F) and GTACCCACTCACTGCCCCGAGG (R).

RNA fluorescence in situ hybridization analysis. Cells seeded on coverslips were transfected with control or siRNAs against ECD and DDX39A, cultured for 72 h, fixed with RNase-free 3.7% formaldehyde, and permeabilized in 70% RNase-free ethanol overnight at 4°C. The coverslips were prehybridized for 5 min (with wash A buffer from the Stellaris, LGC Biosearch Technologies kit) and hybridized with

12.5 μ M oligo(dT) Quasar 570 [22-nucleotide [nt] oligo(dT) custom probe in hybridization buffer; Stellaris, LGC Biosearch Technologies] for 4 h at 37°C in dark. The coverslips were incubated with wash A buffer for 30 min at 37°C in the dark and wash B buffer at room temperature for 5 min, according to the manufacturer's instructions. The coverslips were mounted with Vectashield-DAPI mounting medium and imaged using the LSM 710 confocal microscope under a 63 \times lens. For ErbB2 FISH, we used probe (no. VSMF-2102-5) from Stellaris, LGC Biosearch Technologies. Quantification of nuclear versus cytoplasmic fluorescence was performed using the Intensity Ratio Nuclei Cytoplasm plugin in Image J software.

RNA localization by nuclear/cytoplasmic fractionation of cells. After the specified treatments, cells were trypsinized, counted, and divided into two equal aliquots (one for total RNA isolation and the second for nuclear and cytoplasmic fractionation). Both cell aliquots were lysed on ice in cell lysis buffer for 10 to 20 min. For nuclear/cytoplasmic fractionation, the lysate was centrifuged at 14,000 rpm to collect the nuclear pellet and soluble fraction. The fractions as well as the lysate for total RNA isolation were treated with buffer G (RNA isolation kit cat no. 25501; Active Motif) in 70% ethanol, loaded on to a spin column, and subjected to centrifugation; the retained precipitate was washed with ethanol one time and was eluted in RNase-free water. cDNAs were prepared from various RNA preparations, and qRT-PCR was performed (as mentioned above). mRNAs from nuclear and cytoplasmic fractions were normalized to total RNA isolated from an identical number of cells.

mRNA stability assays. Cells were seeded in 6-well plates (200,000 cells per well). After 48 h of ECD knockdown, actinomycin D (5 μ g/ml) (Sigma, St. Louis, MO) was added at zero time point. Total RNA was isolated at indicated time points (0, 2, 4, 6, 8, and 12 h) after actinomycin D treatment with TRIzol per the manufacturer's protocol. First-strand cDNA was synthesized using SuperScript III reverse transcriptase, followed by qRT-PCR with ErbB2, ECD, and GAPDH primers, as described above.

TCGA and METABRIC database analysis. The ECD mRNA expression analysis in breast cancer tissues was performed using the publicly available fragments per kilobase of transcript per million mapped reads upper quartile (FPKM-UQ) data from The Cancer Genome Atlas (TCGA), downloaded from the Genomic Data Commons (GDC). For the analysis of ECD mRNA expression, the BC TCGA data set comprised 1,089 cases, which were further stratified as 676 cases of ER⁺/PR⁺, 164 cases of HER2⁺, and 112 adjacent normal breast tissue samples based on clinical data. ECD expression in box plots represents the log base 2 (\log_2) values compared to that for adjacent normal tissue, and the significance was calculated using a *t* test. The survival data by multivariate Cox regression analysis of the 854-case TCGA cohort were analyzed as described previously (91). The number of cases analyzed per subgroup is indicated in the Kaplan-Meier plots. Dichotomization of ECD expression was performed using the X-tile software to compare the outcomes (92). For the TCGA data set, 834.2 was used as a cutoff point for high and low ECD mRNA expression. The ECD mRNA expression was also assessed utilizing the Molecular Taxonomy of Breast Cancer International Consortium (METABRIC) cohort (*n* = 1,980) with the clinical-pathological parameters and outcome data available (93). The high and low ECD expression was assigned a cutoff of 7.24 using the X-tile software.

Statistical analysis. Each assay in our study was repeated at least three independent times. Comparisons between two groups were made using *t* tests for continuous outcomes. Comparisons among at least three treatment groups were made using one-way analysis of variance (ANOVA) for continuous outcomes. If the overall tests yielded significant results, *post hoc* tests with Tukey's method for multiple comparisons were conducted. \log_{10} transformations were applied to continuous outcomes to meet ANOVA or *t* test assumptions as necessary. *P* values of ≤ 0.05 were considered statistically significant. Data analysis was performed using SAS version 9.4 (SAS Institute, Cary, NC, USA) and GraphPad Prism. SPSS 24.0 statistical software (SPSS Inc., Chicago, IL, USA) was used for statistical analysis of ECD mRNA expression. Survival curves were analyzed using the Kaplan-Meier analysis with the log rank test. Cox's proportional hazard method was performed for multivariate analysis to identify the independent prognostic value of ECD expression. Spearman correlation coefficients were calculated to analyze the association between continuous variables. The chi-square test was carried out for interrelationships between categorical variables. A *P* value of < 0.05 was considered statistically significant.

SUPPLEMENTAL MATERIAL

Supplemental material is available online only.

SUPPLEMENTAL FILE 1, PDF file, 0.7 MB.

SUPPLEMENTAL FILE 2, PDF file, 1.5 MB.

ACKNOWLEDGMENTS

We acknowledge the University of Nebraska Medical Center confocal and other core facilities.

S.M. was a postdoctoral fellow of the Susan G. Komen Foundation. A.S. and I.S. received graduate fellowships from UNMC. This work was supported by NIH grant R21CA241055 to V.B., Department of Defense grants W81XWH-17-1-0616 and W81XWH-20-1-0058 to H.B. and W81XWH-20-1-0546 to V.B., a Nebraska initiative grant to V.B., and a pilot grant to V.B. from National Cancer Institute Cancer Center support grant P30CA036727 to the Fred and Pamela Buffett Cancer Center, which also supports the University of Nebraska Medical Center

confocal, flow cytometry, and other core facilities, and funding by National Institute of General Medical Sciences grant P30GM1063 and the Nebraska Research Initiative.

We declare no potential conflicts of interest.

V.B. and H.B. conceived and designed the study and analyzed the data. I.S. and S.M. generated the majority of experimental data, analyzed the data, and wrote the draft of the manuscript. V.B. and H.B. edited the manuscript. A.S., M.R., I.M., B.M., M.A.A., and E.A.R. assisted with obtaining experimental data, data analysis, and processing of manuscript images. N.K.M., M.A.A., C.G., and E.A.R. helped in analysis of TCGA and METABRIC data as well as interpretation of the data. F.Q. conducted the statistical analyses. J.H.K. performed affinity purification and mass spec to identify the protein-protein interactome of ECD. All the authors read the manuscript, provided feedback, and approved the final manuscript.

REFERENCES

- Wegener M, Muller-McNicoll M. 2018. Nuclear retention of mRNAs - quality control, gene regulation and human disease. *Semin Cell Dev Biol* 79:131–142. <https://doi.org/10.1016/j.semcdb.2017.11.001>.
- Williams T, Ngo LH, Wickramasinghe VO. 2018. Nuclear export of RNA: different sizes, shapes and functions. *Semin Cell Dev Biol* 75:70–77. <https://doi.org/10.1016/j.semcdb.2017.08.054>.
- Simos G, Hurt E. 1999. Transfer RNA biogenesis: a visa to leave the nucleus. *Curr Biol* 9:R238–R241. [https://doi.org/10.1016/S0960-9822\(99\)80152-3](https://doi.org/10.1016/S0960-9822(99)80152-3).
- Reed R, Hurt E. 2002. A conserved mRNA export machinery coupled to pre-mRNA splicing. *Cell* 108:523–531. [https://doi.org/10.1016/S0092-8674\(02\)00627-X](https://doi.org/10.1016/S0092-8674(02)00627-X).
- Rodriguez-Navarro S, Hurt E. 2011. Linking gene regulation to mRNA production and export. *Curr Opin Cell Biol* 23:302–309. <https://doi.org/10.1016/j.cceb.2010.12.002>.
- Kohler A, Hurt E. 2007. Exporting RNA from the nucleus to the cytoplasm. *Nat Rev Mol Cell Biol* 8:761–773. <https://doi.org/10.1038/nrm2255>.
- Masuda S, Das R, Cheng H, Hurt E, Dorman N, Reed R. 2005. Recruitment of the human TREX complex to mRNA during splicing. *Genes Dev* 19:1512–1517. <https://doi.org/10.1101/gad.1302205>.
- Cullen BR. 2003. Nuclear RNA export. *J Cell Sci* 116:587–597. <https://doi.org/10.1242/jcs.00268>.
- Fabre E, Boelens WC, Wimmer C, Mattaj JW, Hurt EC. 1994. Nup145p is required for nuclear export of mRNA and binds homopolymeric RNA *in vitro* via a novel conserved motif. *Cell* 78:275–289. [https://doi.org/10.1016/0092-8674\(94\)90297-6](https://doi.org/10.1016/0092-8674(94)90297-6).
- Doye V, Wepf R, Hurt EC. 1994. A novel nuclear pore protein Nup133p with distinct roles in poly(A)⁺ RNA transport and nuclear pore distribution. *EMBO J* 13:6062–6075. <https://doi.org/10.1002/j.1460-2075.1994.tb06953.x>.
- Yao W, Roser D, Kohler A, Bradatsch B, Bassler J, Hurt E. 2007. Nuclear export of ribosomal 60S subunits by the general mRNA export receptor Mex67-Mtr2. *Mol Cell* 26:51–62. <https://doi.org/10.1016/j.molcel.2007.02.018>.
- Wiegand HL, Coburn GA, Zeng Y, Kang Y, Bogerd HP, Cullen BR. 2002. Formation of Tap/NXT1 heterodimers activates Tap-dependent nuclear mRNA export by enhancing recruitment to nuclear pore complexes. *Mol Cell Biol* 22:245–256. <https://doi.org/10.1128/mcb.22.1.245-256.2002>.
- Truant R, Kang Y, Cullen BR. 1999. The human tap nuclear RNA export factor contains a novel transportin-dependent nuclear localization signal that lacks nuclear export signal function. *J Biol Chem* 274:32167–32171. <https://doi.org/10.1074/jbc.274.45.32167>.
- Katahira J, Inoue H, Hurt E, Yoneda Y. 2009. Adaptor Aly and co-adaptor Thoc5 function in the Tap-p15-mediated nuclear export of HSP70 mRNA. *EMBO J* 28:556–567. <https://doi.org/10.1038/emboj.2009.5>.
- Kang Y, Cullen BR. 1999. The human Tap protein is a nuclear mRNA export factor that contains novel RNA-binding and nucleocytoplasmic transport sequences. *Genes Dev* 13:1126–1139. <https://doi.org/10.1101/gad.13.9.1126>.
- Kang Y, Bogerd HP, Yang J, Cullen BR. 1999. Analysis of the RNA binding specificity of the human tap protein, a constitutive transport element-specific nuclear RNA export factor. *Virology* 262:200–209. <https://doi.org/10.1006/viro.1999.9906>.
- Cullen BR. 2003. Nuclear mRNA export: insights from virology. *Trends Biochem Sci* 28:419–424. [https://doi.org/10.1016/S0968-0004\(03\)00142-7](https://doi.org/10.1016/S0968-0004(03)00142-7).
- Hutten S, Kehlenbach RH. 2007. CRM1-mediated nuclear export: to the pore and beyond. *Trends Cell Biol* 17:193–201. <https://doi.org/10.1016/j.tcb.2007.02.003>.
- Hurt E, Strasser K, Segref A, Bailer S, Schlaich N, Presutti C, Tollervey D, Jansen R. 2000. Mex67p mediates nuclear export of a variety of RNA polymerase II transcripts. *J Biol Chem* 275:8361–8368. <https://doi.org/10.1074/jbc.275.12.8361>.
- Katahira J, Strasser K, Podtelejnikov A, Mann M, Jung JU, Hurt E. 1999. The Mex67p-mediated nuclear mRNA export pathway is conserved from yeast to human. *EMBO J* 18:2593–2609. <https://doi.org/10.1093/emboj/18.9.2593>.
- Santos-Rosa H, Moreno H, Simos G, Segref A, Fahrenkrog B, Pante N, Hurt E. 1998. Nuclear mRNA export requires complex formation between Mex67p and Mtr2p at the nuclear pores. *Mol Cell Biol* 18:6826–6838. <https://doi.org/10.1128/mcb.18.11.6826>.
- Segref A, Sharma K, Doye V, Hellwig A, Huber J, Luhrmann R, Hurt E. 1997. Mex67p, a novel factor for nuclear mRNA export, binds to both poly(A)⁺ RNA and nuclear pores. *EMBO J* 16:3256–3271. <https://doi.org/10.1093/emboj/16.11.3256>.
- Gallouzi IE, Brennan CM, Steitz JA. 2001. Protein ligands mediate the CRM1-dependent export of HuR in response to heat shock. *RNA* 7:1348–1361. <https://doi.org/10.1017/s1355838201016089>.
- Topisirovic I, Siddiqui N, Lapointe VL, Trost M, Thibault P, Bangeranye C, Pinol-Roma S, Borden KL. 2009. Molecular dissection of the eukaryotic initiation factor 4E (eIF4E) export-competent RNP. *EMBO J* 28:1087–1098. <https://doi.org/10.1038/emboj.2009.53>.
- Cullen BR. 2004. Assaying nuclear messenger RNA export in human cells. *Methods Mol Biol* 257:85–92. <https://doi.org/10.1385/1-59259-750-5:085>.
- Wickramasinghe VO, Stewart M, Laskey RA. 2010. GANP enhances the efficiency of mRNA nuclear export in mammalian cells. *Nucleus* 1:393–396. <https://doi.org/10.4161/nucl.1.5.12351>.
- Wickramasinghe VO, Andrews R, Ellis P, Langford C, Gurdon JB, Stewart M, Venkitaraman AR, Laskey RA. 2014. Selective nuclear export of specific classes of mRNA from mammalian nuclei is promoted by GANP. *Nucleic Acids Res* 42:5059–5071. <https://doi.org/10.1093/nar/gku095>.
- Sakakibara K, Saito N, Sato T, Suzuki A, Hasegawa Y, Friedman JM, Kufe DW, Vonnhoff DD, Iwami T, Kawabe T. 2011. CBS9106 is a novel reversible oral CRM1 inhibitor with CRM1 degrading activity. *Blood* 118:3922–3931. <https://doi.org/10.1182/blood-2011-01-333138>.
- van der Watt PJ, Zemanay W, Govender D, Hendricks DT, Parker MI, Leaner VD. 2014. Elevated expression of the nuclear export protein, Crm1 (exportin 1), associates with human oesophageal squamous cell carcinoma. *Oncol Rep* 32:730–738. <https://doi.org/10.3892/or.2014.3231>.
- Claudius AK, Romani P, Lamkemeyer T, Jindra M, Uhlirava M. 2014. Unexpected role of the steroid-deficiency protein ecdysoneless in pre-mRNA splicing. *PLoS Genet* 10:e1004287. <https://doi.org/10.1371/journal.pgen.1004287>.
- Kim JH, Gurumurthy CB, Naramura M, Zhang Y, Dudley AT, Doglio L, Band H, Band V. 2009. Role of mammalian ecdysoneless in cell cycle regulation. *J Biol Chem* 284:26402–26410. <https://doi.org/10.1074/jbc.M109.030551>.
- Olou AA, Sarkar A, Bele A, Gurumurthy CB, Mir RA, Ammons SA, Mirza S, Saleem I, Urano F, Band H, Band V. 2017. Mammalian ECD protein is a novel negative regulator of the PERK arm of the unfolded protein response. *Mol Cell Biol* 37:e00030-17. <https://doi.org/10.1128/MCB.00030-17>.

33. Mir RA, Lovelace J, Schafer NP, Simone PD, Kellezi A, Kolar C, Spagnol G, Sorgen PL, Band H, Band V, Borgstahl GEO. 2016. Biophysical characterization and modeling of human Ecdysoneless (ECD) protein supports a scaffolding function. *AIMS Biophys* 3:195–208. <https://doi.org/10.3934/biophys.2016.1.195>.
34. Cloutier P, Poitras C, Durand M, Hekmat O, Fiola-Masson É, Bouchard A, Faubert D, Chabot B, Coulombe B. 2017. R2TP/prefoldin-like component RUVBL1/RUVBL2 directly interacts with ZNHIT2 to regulate assembly of U5 small nuclear ribonucleoprotein. *Nat Commun* 8:15615. <https://doi.org/10.1038/ncomms15615>.
35. Malinova A, Cvackova Z, Mateju D, Horejsi Z, Abeza C, Vandermoere F, Bertrand E, Stanek D, Verheggen C. 2017. Assembly of the U5 snRNP component PRPF8 is controlled by the HSP90/R2TP chaperones. *J Cell Biol* 216:1579–1596. <https://doi.org/10.1083/jcb.201701165>.
36. Horejsi Z, Stach L, Flower TG, Joshi D, Flynn H, Skehel JM, O'Reilly NJ, Ogrodowicz RW, Smerdon SJ, Boulton SJ. 2014. Phosphorylation-dependent PIH1D1 interactions define substrate specificity of the R2TP cochaperone complex. *Cell Rep* 7:19–26. <https://doi.org/10.1016/j.celrep.2014.03.013>.
37. Mir RA, Bele A, Mirza S, Srivastava S, Olou AA, Ammons SA, Kim JH, Gurumurthy CB, Qiu F, Band H, Band V. 2015. A novel interaction of ecdysoneless (ECD) protein with R2TP complex component RUVBL1 is required for the functional role of ECD in cell cycle progression. *Mol Cell Biol* 36:886–899. <https://doi.org/10.1128/MCB.00594-15>.
38. Dey P, Rachagani S, Chakraborty S, Singh PK, Zhao X, Gurumurthy CB, Anderson JM, Lele S, Hollingsworth MA, Band V, Batra SK. 2012. Overexpression of ecdysoneless in pancreatic cancer and its role in oncogenesis by regulating glycolysis. *Clin Cancer Res* 18:6188–6198. <https://doi.org/10.1158/1078-0432.CCR-12-1789>.
39. Zhao X, Mirza S, Alshareeda A, Zhang Y, Gurumurthy CB, Bele A, Kim JH, Mohibi S, Goswami M, Lele SM, West W, Qiu F, Ellis IO, Rakha EA, Green AR, Band H, Band V. 2012. Overexpression of a novel cell cycle regulator ecdysoneless in breast cancer: a marker of poor prognosis in HER2/neu-overexpressing breast cancer patients. *Breast Cancer Res Treat* 134:171–180. <https://doi.org/10.1007/s10549-011-1946-8>.
40. Xu SH, Huang JZ, Xu ML, Yu G, Yin XF, Chen D, Yan GR. 2015. ACK1 promotes gastric cancer epithelial-mesenchymal transition and metastasis through AKT-POU2F1-ECD signalling. *J Pathol* 236:175–185. <https://doi.org/10.1002/path.4515>.
41. Xu SH, Huang JZ, Chen M, Zeng M, Zou FY, Chen D, Yan GR. 2017. Amplification of ACK1 promotes gastric tumorigenesis via ECD-dependent p53 ubiquitination degradation. *Oncotarget* 8:12705–12716. <https://doi.org/10.18632/oncotarget.6194>.
42. Bele A, Mirza S, Zhang Y, Ahmad Mir R, Lin S, Kim JH, Gurumurthy CB, West W, Qiu F, Band H, Band V. 2015. The cell cycle regulator ecdysoneless cooperates with H-Ras to promote oncogenic transformation of human mammary epithelial cells. *Cell Cycle* 14:990–1000. <https://doi.org/10.1080/15384101.2015.1006982>.
43. Thomas M, Lischka P, Muller R, Stamminger T. 2011. The cellular DExD/H-box RNA-helicases UAP56 and URH49 exhibit a CRM1-independent nucleocytoplasmic shuttling activity. *PLoS One* 6:e22671. <https://doi.org/10.1371/journal.pone.0022671>.
44. Luo ML, Zhou Z, Zhang X, Christoforides C, Rappsilber J, Mann M, Reed R. 2001. Pre-mRNA splicing and mRNA export linked by direct interactions between UAP56 and Aly. *Nature* 413:644–647. <https://doi.org/10.1038/35098106>.
45. Yamazaki T, Fujiwara N, Yukinaga H, Ebisuya M, Shiki T, Kurihara T, Kioka N, Kambe T, Nagao M, Nishida E, Masuda S. 2010. The closely related RNA helicases, UAP56 and URH49, preferentially form distinct mRNA export machineries and coordinately regulate mitotic progression. *Mol Biol Cell* 21:2953–2965. <https://doi.org/10.1091/mbc.E09-10-0913>.
46. Nakata D, Nakao S, Nakayama K, Araki S, Nakayama Y, Aparicio S, Hara T, Nakanishi A. 2017. The RNA helicase DDX39B and its paralog DDX39A regulate androgen receptor splice variant AR-V7 generation. *Biochem Biophys Res Commun* 483:271–276. <https://doi.org/10.1016/j.bbrc.2016.12.153>.
47. Fujita KI, Yamazaki T, Harada K, Seno S, Matsuda H, Masuda S. 2020. URH49 exports mRNA by remodeling complex formation and mediating the NXF1-dependent pathway. *Biochim Biophys Acta Gene Regul Mech* 1863:194480. <https://doi.org/10.1016/j.bbagr.2020.194480>.
48. Zhang Y, Chen J, Gurumurthy CB, Kim J, Bhat I, Gao Q, Dimri G, Lee SW, Band H, Band V. 2006. The human orthologue of *Drosophila* ecdysoneless protein interacts with p53 and regulates its function. *Cancer Res* 66:7167–7175. <https://doi.org/10.1158/0008-5472.CAN-06-0722>.
49. Sugiura T, Sakurai K, Nagano Y. 2007. Intracellular characterization of DDX39, a novel growth-associated RNA helicase. *Exp Cell Res* 313:782–790. <https://doi.org/10.1016/j.yexcr.2006.11.014>.
50. Gaziouva I, Bonnette PC, Henrich VC, Jindra M. 2004. Cell-autonomous roles of the ecdysoneless gene in *Drosophila* development and oogenesis. *Development* 131:2715–2725. <https://doi.org/10.1242/dev.01143>.
51. Kim JH, Gurumurthy CB, Band H, Band V. 2010. Biochemical characterization of human ecdysoneless reveals a role in transcriptional regulation. *Biol Chem* 391:9–19. <https://doi.org/10.1515/BC.2010.004>.
52. Hautbergue GM, Hung ML, Walsh MJ, Snijders AP, Chang CT, Jones R, Ponting CP, Dickman MJ, Wilson SA. 2009. UIF, a new mRNA export adaptor that works together with REF/ALY, requires FACT for recruitment to mRNA. *Curr Biol* 19:1918–1924. <https://doi.org/10.1016/j.cub.2009.09.041>.
53. Slamon DJ, Godolphin W, Jones LA, Holt JA, Wong SG, Keith DE, Levin WJ, Stuart SG, Udove J, Ullrich A, et al. 1989. Studies of the HER-2/neu proto-oncogene in human breast and ovarian cancer. *Science* 244:707–712. <https://doi.org/10.1126/science.2470152>.
54. Pasleau F, Grootclaes M, Gol-Winkler R. 1993. Expression of the *c-erbB2* gene in the BT474 human mammary tumor cell line: measurement of *c-erbB2* mRNA half-life. *Oncogene* 8:849–854.
55. Awasthi S, Hamburger AW. 2014. Heregulin negatively regulates transcription of ErbB2/3 receptors via an AKT-mediated pathway. *J Cell Physiol* 229:1831–1841. <https://doi.org/10.1002/jcp.24637>.
56. Siegel PM, Ryan ED, Cardiff RD, Muller WJ. 1999. Elevated expression of activated forms of Neu/ErbB-2 and ErbB-3 are involved in the induction of mammary tumors in transgenic mice: implications for human breast cancer. *EMBO J* 18:2149–2164. <https://doi.org/10.1093/emboj/18.8.2149>.
57. Castiglioni F, Tagliabue E, Campiglio M, Pupa SM, Balsari A, Menard S. 2006. Role of exon-16-deleted HER2 in breast carcinomas. *Endocr Relat Cancer* 13:221–232. <https://doi.org/10.1677/erc.1.01047>.
58. Doherty JK, Bond C, Jardim A, Adelman JP, Clinton GM. 1999. The HER-2/neu receptor tyrosine kinase gene encodes a secreted autoinhibitor. *Proc Natl Acad Sci U S A* 96:10869–10874. <https://doi.org/10.1073/pnas.96.19.10869>.
59. Azios NG, Romero FJ, Denton MC, Doherty JK, Clinton GM. 2001. Expression of herstatin, an autoinhibitor of HER-2/neu, inhibits transactivation of HER-3 by HER-2 and blocks EGF activation of the EGF receptor. *Oncogene* 20:5199–5209. <https://doi.org/10.1038/sj.onc.1204555>.
60. Siliipo M, Gautrey H, Satam S, Lennard T, Tyson-Capper A. 2017. How is herstatin, a tumor suppressor splice variant of the oncogene HER2, regulated? *RNA Biol* 14:536–543. <https://doi.org/10.1080/15476286.2016.1267074>.
61. Alajati A, Sausgruber N, Aceto N, Duss S, Sarret S, Voshol H, Bonenfant D, Bentires-Alj M. 2013. Mammary tumor formation and metastasis evoked by a HER2 splice variant. *Cancer Res* 73:5320–5327. <https://doi.org/10.1158/0008-5472.CAN-12-3186>.
62. Kwong KY, Hung MC. 1998. A novel splice variant of HER2 with increased transformation activity. *Mol Carcinog* 23:62–68. [https://doi.org/10.1002/\(SICI\)1098-2744\(199810\)23:2<62::AID-MC2>3.0.CO;2-O](https://doi.org/10.1002/(SICI)1098-2744(199810)23:2<62::AID-MC2>3.0.CO;2-O).
63. Miyagawa R, Tano K, Mizuno R, Nakamura Y, Ijiri K, Rakwal R, Shibata J, Masuo Y, Mayeda A, Hirose T, Akimitsu N. 2012. Identification of *cis*- and *trans*-acting factors involved in the localization of MALAT-1 noncoding RNA to nuclear speckles. *RNA* 18:738–751. <https://doi.org/10.1261/rna.028639.111>.
64. Stubbs SH, Conrad NK. 2015. Depletion of REF/Aly alters gene expression and reduces RNA polymerase II occupancy. *Nucleic Acids Res* 43:504–519. <https://doi.org/10.1093/nar/gku1278>.
65. Stubbs SH, Hunter OV, Hoover A, Conrad NK. 2012. Viral factors reveal a role for REF/Aly in nuclear RNA stability. *Mol Cell Biol* 32:1260–1270. <https://doi.org/10.1128/MCB.06420-11>.
66. Volpon L, Culjkovic-Kraljacic B, Sohn HS, Blanchet-Cohen A, Osborne MJ, Borden KLB. 2017. A biochemical framework for eIF4E-dependent mRNA export and nuclear recycling of the export machinery. *RNA* 23:927–937. <https://doi.org/10.1261/rna.060137.116>.
67. Hurt JA, Silver PA. 2008. mRNA nuclear export and human disease. *Dis Model Mech* 1:103–108. <https://doi.org/10.1242/dmm.000745>.
68. Munoz-Hernandez H, Pal M, Rodriguez CF, Prodromou C, Pearl LH, Llorca O. 2018. Advances on the structure of the R2TP/prefoldin-like complex. *Adv Exp Med Biol* 1106:73–83. https://doi.org/10.1007/978-3-030-00737-9_5.
69. Boulon S, Pradet-Balade B, Verheggen C, Molle D, Boireau S, Georgieva M, Azzag K, Robert MC, Ahmad Y, Neel H, Lamond AI, Bertrand E. 2010. HSP90 and its R2TP/prefoldin-like cochaperone are involved in the

- cytoplasmic assembly of RNA polymerase II. *Mol Cell* 39:912–924. <https://doi.org/10.1016/j.molcel.2010.08.023>.
70. Kakiyama Y, Saeki M. 2014. The R2TP chaperone complex: its involvement in snoRNP assembly and tumorigenesis. *Biomol Concepts* 5:513–520. <https://doi.org/10.1515/bmc-2014-0028>.
 71. Kakiyama Y, Houry WA. 2012. The R2TP complex: discovery and functions. *Biochim Biophys Acta* 1823:101–107. <https://doi.org/10.1016/j.bbamcr.2011.08.016>.
 72. Verheggen C, Pradet-Balade B, Bertrand E. 2015. SnoRNPs, ZNHIT proteins and the R2TP pathway. *Oncotarget* 6:41399–41400. <https://doi.org/10.18632/oncotarget.6388>.
 73. Yu G, Zhao Y, Tian S, Rai J, He H, Spear J, Sousa D, Fan J, Yu HG, Stagg SM, Li H. 2019. Yeast R2TP interacts with extended termini of client protein Nop58p. *Sci Rep* 9:20228. <https://doi.org/10.1038/s41598-019-56712-4>.
 74. Siddiqui N, Borden KL. 2012. mRNA export and cancer. *Wiley Interdiscip Rev RNA* 3:13–25. <https://doi.org/10.1002/wrna.101>.
 75. Kikuta K, Kubota D, Saito T, Orita H, Yoshida A, Tsuda H, Suehara Y, Katai H, Shimada Y, Toyama Y, Sato K, Yao T, Kaneko K, Beppu Y, Murakami Y, Kawai A, Kondo T. 2012. Clinical proteomics identified ATP-dependent RNA helicase DDX39 as a novel biomarker to predict poor prognosis of patients with gastrointestinal stromal tumor. *J Proteomics* 75:1089–1098. <https://doi.org/10.1016/j.jprot.2011.10.005>.
 76. Kato M, Wei M, Yamano S, Kakehashi A, Tamada S, Nakatani T, Wanibuchi H. 2012. DDX39 acts as a suppressor of invasion for bladder cancer. *Cancer Sci* 103:1363–1369. <https://doi.org/10.1111/j.1349-7006.2012.02298.x>.
 77. Zhang T, Ma Z, Liu L, Sun J, Tang H, Zhang B, Zou Y, Li H. 2018. DDX39 promotes hepatocellular carcinoma growth and metastasis through activating Wnt/beta-catenin pathway. *Cell Death Dis* 9:675. <https://doi.org/10.1038/s41419-018-0591-0>.
 78. Sugiura T, Nagano Y, Noguchi Y. 2007. DDX39, upregulated in lung squamous cell cancer, displays RNA helicase activities and promotes cancer cell growth. *Cancer Biol Ther* 6:957–964. <https://doi.org/10.4161/cbt.6.6.4192>.
 79. Otake K, Uchida K, Ide S, Kobayashi Y, Kobayashi I, Kusunoki M. 2016. Identification of DDX39A as a potential biomarker for unfavorable neuroblastoma using a proteomic approach. *Pediatr Blood Cancer* 63:221–227. <https://doi.org/10.1002/pbc.25778>.
 80. Ma J, Chang W, Zhang W. 2018. Relationship between the expression of DDX39 protein and prognosis of colorectal cancer. *Zhonghua Wei Chang Wai Ke Za Zhi* 21:336–341. (In Chinese.)
 81. Culjkovic-Kraljacic B, Borden KL. 2013. Aiding and abetting cancer: mRNA export and the nuclear pore. *Trends Cell Biol* 23:328–335. <https://doi.org/10.1016/j.tcb.2013.03.004>.
 82. Marotta M, Onodera T, Johnson J, Budd GT, Watanabe T, Cui X, Giuliano AE, Niida A, Tanaka H. 2017. Palindromic amplification of the ERBB2 oncogene in primary HER2-positive breast tumors. *Sci Rep* 7:41921. <https://doi.org/10.1038/srep41921>.
 83. Tudek A, Schmid M, Makaras M, Barras JD, Beggs JD, Jensen TH. 2018. A nuclear export block triggers the decay of newly synthesized polyadenylated RNA. *Cell Rep* 24:2457.e7–2467.e7. <https://doi.org/10.1016/j.celrep.2018.07.103>.
 84. Mitra D, Brumlik MJ, Okamgba SU, Zhu Y, Duplessis TT, Parvani JG, Lesko SM, Brogi E, Jones FE. 2009. An oncogenic isoform of HER2 associated with locally disseminated breast cancer and trastuzumab resistance. *Mol Cancer Ther* 8:2152–2162. <https://doi.org/10.1158/1535-7163.MCT-09-0295>.
 85. Yoo HH, Chung IK. 2011. Requirement of DDX39 DEAD box RNA helicase for genome integrity and telomere protection. *Aging Cell* 10:557–571. <https://doi.org/10.1111/j.1474-9726.2011.00696.x>.
 86. Kronemann D, Hagemeyer SR, Cygnar D, Phillips S, Bresnahan WA. 2010. Binding of the human cytomegalovirus (HCMV) tegument protein UL69 to UAP56/URH49 is not required for efficient replication of HCMV. *J Virol* 84:9649–9654. <https://doi.org/10.1128/JVI.00669-10>.
 87. Pryor A, Tung L, Yang Z, Kapadia F, Chang TH, Johnson LF. 2004. Growth-regulated expression and G0-specific turnover of the mRNA that encodes URH49, a mammalian DExH/D box protein that is highly related to the mRNA export protein UAP56. *Nucleic Acids Res* 32:1857–1865. <https://doi.org/10.1093/nar/gkh347>.
 88. Majerciak V, Deng M, Zheng ZM. 2010. Requirement of UAP56, URH49, RBM15, and OTT3 in the expression of Kaposi sarcoma-associated herpesvirus ORF57. *Virology* 407:206–212. <https://doi.org/10.1016/j.virol.2010.08.014>.
 89. Mohibi S, Srivastava S, Bele A, Mirza S, Band H, Band V. 2016. Acetylation of mammalian ADA3 is required for its functional roles in histone acetylation and cell proliferation. *Mol Cell Biol* 36:2487–2502. <https://doi.org/10.1128/MCB.00342-16>.
 90. Bhagirath D, Zhao X, West WW, Qiu F, Band H, Band V. 2015. Cell type of origin as well as genetic alterations contribute to breast cancer phenotypes. *Oncotarget* 6:9018–9030. <https://doi.org/10.18632/oncotarget.3379>.
 91. Kurozumi S, Joseph C, Sonbul S, Alsaeed S, Kariri Y, Aljohani A, Raafat S, Alsaleem M, Ogden A, Johnston SJ, Aleskandarany MA, Fujii T, Shirabe K, Caldas C, Ashankyty I, Dalton L, Ellis IO, Desmedt C, Green AR, Mongan NP, Rakha EA. 2019. A key genomic subtype associated with lymphovascular invasion in invasive breast cancer. *Br J Cancer* 120:1129–1136. <https://doi.org/10.1038/s41416-019-0486-6>.
 92. Camp RL, Dolled-Filhart M, Rimm DL. 2004. X-tile: a new bio-informatics tool for biomarker assessment and outcome-based cut-point optimization. *Clin Cancer Res* 10:7252–7259. <https://doi.org/10.1158/1078-0432.CCR-04-0713>.
 93. Curtis C, Shah SP, Chin SF, Turashvili G, Rueda OM, Dunning MJ, Speed D, Lynch AG, Samarajiwa S, Yuan Y, Graf S, Ha G, Haffari G, Bashashati A, Russell R, McKinney S, METABRIC Group, Langerod A, Green A, Provenzano E, Wishart G, Pinder S, Watson P, Markowitz F, Murphy L, Ellis I, Purushotham A, Borresen-Dale AL, Brenton JD, Tavare S, Caldas C, Aparicio S. 2012. The genomic and transcriptomic architecture of 2,000 breast tumours reveals novel subgroups. *Nature* 486:346–352. <https://doi.org/10.1038/nature10983>.